Chemical Science

MINIREVIEW

View Article Online
View Journal | View Issue

Cite this: *Chem. Sci.*, 2017, **8**, 7339

Molecular design of upconversion nanoparticles for gene delivery

Wing-Fu Lai, *[ab] Andrey L. Rogach [c] and Wing-Tak Wong *[b]

Received 6th July 2017
Accepted 29th August 2017

DOI: 10.1039/c7sc02956j

rsc.li/chemical-science

Due to their large anti-Stokes shifts, sharp emission spectra and long excited-state lifetimes, upconversion nanoparticles (UCNPs) have attracted an increasing amount of research interests, and have shown great potential for enhancing the practical utility of gene therapy, whose versatility has been limited by existing gene delivery technologies that are basically mono-functional in nature. Despite this, up to now in-depth analysis of the development of UCNPs for gene delivery has been scant in the literature, even though there has been an upsurge of reviews on the chemistry of UCNPs and their applications in bioimaging and drug delivery. To fill this gap, this review aims to present the latest advances in the development and applications of UCNPs as gene carriers. Prior to describing the prominent works published in the field, a critical view on the properties, chemistry and molecular design of UCNPs for gene delivery is provided. With a synopsis of the recent advances in UCNP-mediated gene delivery, challenges and opportunities could be illuminated for clinical translation of works in this nascent field of research.

1. Introduction

Current research in gene delivery has reached a bottle-neck in terms of efficiency and versatility. Hopes to change this situation may now be brought about by the emergence of photobiology, which not only enables imaging during gene therapy but also makes the precise control of the timing and location of the release of the loaded gene possible. To achieve this goal, over the years, different optically-active materials have been developed, ranging from quantum dots (QDs) to luminescent transition metal complexes. Each of them has their own merits and drawbacks in applications (Table 1).[1–10] Among them, upconversion nanoparticles (UCNPs) have attracted extensive research interests and represent a hot topic in materials chemistry. Compared to the conventional down-

[a]School of Pharmaceutical Sciences, Health Science Centre, Shenzhen University, Shenzhen, China

[b]Department of Applied Biology & Chemical Technology, The Hong Kong Polytechnic University, Hong Kong. E-mail: rori0610@graduate.hku.hk; w.t.wong@polyu.edu.hk

[c]Department of Materials Science and Engineering & Centre for Functional Photonics (CFP), City University of Hong Kong, Hong Kong

Wing-Fu Lai received his MSc degree in Materials Engineering and Nanotechnology from the City University of Hong Kong, and earned his PhD in Chemistry from the University of Hong Kong. He joined the faculty of the School of Pharmaceutical Sciences at Shenzhen University in 2016, and is also holding an adjunct assistant professorship in the Department of Applied Biology and Chemical Technology at the Hong Kong Polytechnic University. His research interests cover the design of molecular probes for bioimaging, the synthesis of polymeric materials for gene delivery and controlled drug release, and the development of nanoparticulate systems for theranostic applications.

Andrey L. Rogach is a Chair Professor of Photonics Materials and the founding director of the Centre for Functional Photonics at the City University of Hong Kong. He received his Ph.D. in Physical Chemistry (1995) from the Belarusian State University in Minsk, and worked as a staff scientist at the University of Hamburg, Germany, from 1995 to 2002. During 2002–2009, he held the tenured position of lead staff scientist at the Department of Physics of the Ludwig-Maximilians-University in Munich, Germany, where he completed his habilitation in Experimental Physics. His research focuses on light-emitting materials, in particular for bioimaging applications.

conversion fluorophores, UCNPs have several optical properties favourable for biomedical use, including negligible photobleaching and photoblinking, lower interference from auto-fluorescence from surrounding tissues, higher spatial resolution, and less photodamage caused by the excitation light to fragile biological molecules.

Since the turn of the last century, the focus of research on UCNPs has been shifted from the controlled synthesis of uniform nanoparticles to exploration of biomedical applications.[11–14] In recent years, the potential of UCNPs has begun to receive considerable attention as a new approach to enhance the versatility of gene therapy. Unfortunately, up to now discussions on the emerging yet encouraging potential of UCNPs in gene delivery have been scant in the literature. This leaves a strong demand for a review filling this gap. The objective of this article is to meet this need by reviewing the latest development of UCNPs as gene carriers. It is hoped that by offering an outlook of current advances in this burgeoning area of research, further development can be facilitated by avoiding potential duplicate efforts, by enabling the identification of challenges to be met, and by pointing to clearer directions for clinical translation of works on UCNP-based gene delivery in the future.

2. Overview of the properties of UCNPs

Rare earth elements consist of yttrium, scandium and the fifteen elements in the lanthanide series. Except lanthanum and lutetium, the ions of all other lanthanides exhibit distinctive luminescence properties due to possible intra-4f or 4f–5d transitions led by the unique energy structures resulting from the $4f^n$ inner shell configuration.[15,16] Contrary to conventional fluorophores that show downconversion caused by internal energy loss, UCNPs emit higher-energy outcome photons through sequential absorption of lower-energy incident ones.[17] This process is called upconversion, which can be mediated using the long-lived and real ladder-like energy levels of lanthanide ions embedded in an inorganic matrix host.

Wing-Tak Wong, PhD, ScD, is a Chair Professor of Chemical Technology and Dean of Faculty of Applied Science and Textiles at the Hong Kong Polytechnic University. His research interest includes lanthanide chemistry, nanomaterials and bio-imaging. He has published more than 480 research papers and contributed two book chapters in Comprehensive Organometallic Chemistry III (Elsevier 2006) and a book chapter in Rare Earth Coordination Chemistry (Wiley 2010). He is also a co-editor of the book The Chemistry of Molecular Imaging (Wiley 2015).

Upconversion is a non-linear anti-Stokes process that is achieved mainly by three major mechanisms: excited-state absorption (ESA), energy transfer upconversion (ETU), and photon avalanche (PA). PA is rarely found in lanthanide materials at the nanoscale. Its importance to UCNP-based gene carriers, therefore, is less significant. On the other hand, ETU is one of the commonly adopted mechanisms to achieve high upconversion efficiency in practice. During the process, a pump photon of the same energy is absorbed by each of the two neighbouring ions. The subsequent non-radiative energy transfer causes one of the ions to get excited to the upper energy level whereas the other one relaxes back to the ground state. The emission of photons with higher energy results from the relaxation of the excited ion. ETU can be achieved in a number of ways (Fig. 1), including energy transfer followed by excited-state absorption, successive energy transfer, cross-relaxation upconversion, cooperative sensitization and cooperative luminescence. As the mechanisms of luminescence emission from UCNPs have been reviewed elsewhere, readers are referred to those reviews for details.[18–21]

UCNPs generally consist of two parts: (i) trivalent lanthanide dopant ions and (ii) the inorganic host lattice that accommodates those ions. To enhance the upconversion emission, the host lattice has to be carefully selected. This involves consideration of several criteria.[22] For instance, the photon vibration energies shall be low. High chemical stability and close lattice matches to dopant ions are also required. Taking these criteria into account, fluorides (*e.g.*, $NaYF_4$) and oxides (*e.g.*, Y_2O_3, La_2O_3 and Lu_2O_3) are some of the materials favourable to be used as host lattices for UCNP fabrication.[23–27] Apart from the selection of the host lattice, the choice of the dopant ions matters. In general, two types of dopant ions are required. One is the activator which emits visible light; whereas the other one functions as a sensitizer that donates energy. Some host-dopant systems commonly adopted for UCNP synthesis are listed in Table 2.[23,25,28–38] To improve the upconversion luminescence (UCL) efficiency of UCNPs, conventionally it is thought that the concentration of the sensitizer should be higher (approximately 20 mol%) than that of the activator, whose concentration has often been controlled to be below 2 mol% to reduce luminescence quenching.[16] The validity of this conventional wisdom has recently been challenged by Johnson *et al.*,[39] who have discovered that even if the Er^{3+} concentration in $NaY(Er)F_4$/$NaLuF_4$ core–shell nanocrystals is as high as 100 mol%, the emission intensity of both upconversion and downshifted luminescence can still be enhanced, with no significant concentration quenching effects being observed. This suggests that surface quenching rather than cross-relaxation between dopant ions may play a predominate role in causing luminescence quenching at high dopant concentrations.[39] This finding has revealed the possibility of constructing and engineering UCNPs in a way that is no longer restrained by the conventional limit of the activator concentration.

UCNPs are indeed only one of the many luminescent nanoparticles investigated in photobiology. Other nanoparticles widely studied for biomedical applications include transition metal complexes, QDs and organic fluorophores. Compared to

Table 1 A comparison of major classes of luminescent materials used in biomedical applications

Type	Strengths	Drawbacks	Examples	Ref.
Transition metal complexes	• Good aqueous solubility	• High toxicity	Cationic iridium(III) complexes, which can emit green and red light, have been reported as phosphorescent dyes for live cell imaging	1
	• Large Stokes shifts	• Interference from auto-fluorescence from surrounding tissues	Luminescent cyclometalated iridium(III)polypyridine indole complexes have been synthesized, and have been found to emit intense and long-lived luminescence upon photoexcitation in fluid solutions at 298 K or in alcohol glass at 77 K	2
	• Absence of dye–dye interactions	• Attenuation of imaging signals during deep tissue imaging		
Gold nanoparticles	• Good biocompatibility	• Low contrast	Multi-branched gold nanoparticles have been fabricated by reducing tetrachloroauric acid with Tris base, and have been adopted as a substrate for imaging kidney cells based on surface-enhanced Raman scattering (SERS)	3
	• Low toxicity	• Attenuation of imaging signals during deep tissue imaging	Ru(II)-polypyridyl surface-functionalised gold nanoparticles have been reported as an imaging probe that shows targeting capacity towards DNA molecules	4
Quantum dots (QDs)	• Narrow emission bands	• Attenuation of imaging signals during deep tissue imaging	Near infrared (NIR) QDs have been designed. Their applications in monitoring changes in the Cu^{2+} concentration through *in vitro* and *in vivo* fluorescent imaging have been reported	5
	• Tuneable emission properties	• High toxicity	A polysaccharide-QD conjugate has been adopted to generate supramolecular nanoparticles for imaging cancer cells	6
Organic fluorophores	• High quantum efficiency	• Interference from auto-fluorescence from surrounding tissues	Halo tag-based target-specific azidos have been fabricated as photoactivatable organic fluorophores for super-resolution imaging of target proteins in fixed and living cells	7
		• Photobleaching • Photoblinking	Resveratrone glucoside has been synthesized from resveratrol-3-β-mono-D-glucoside *via* photoreactions. The compound has been reported to display a high fluorescence quantum yield, a large Stokes shift, and a large two-photon absorption cross-section	8

Table 1 (*Contd.*)

Type	Strengths	Drawbacks	Examples	Ref.
UCNPs	• Good biocompatibility	• Low extinction coefficient	$NaYF_4$:Yb,Er UCNPs with 6-phosphate-6-deoxy-β-cyclodextrin as the surface ligand have been generated. Cyclic RGD-conjugated adamantine has been incorporated into the UCNP surface for targeted cellular imaging	9
	• Large anti-Stokes shifts • Non-photobleaching • Non-photoblinking • Lower interference from auto-fluorescence from surrounding tissues	• Low quantum yield	Adamantaneacetic acid-capped UCNPs have complexed with β-cyclodextrin. The nanoparticles generated have been shown to give intense upconversion luminescence (UCL) emission after cellular internalization	10

many of these materials, UCNPs have the merit of low toxicity in *in vitro* and *in vivo* contexts. This has been evidenced in the literature,[40–47] in which different concentrations of UCNPs (from 5 to 2500 μg mL^{-1}) and incubation periods (from 2 hour to 48 hours) have been investigated in various cell lines (*e.g.*, HeLa, KB, L929, CL, HCCHM3 and HepG2). Most of these studies have reported that over 75% of cell viability remains after treatment with UCNPs. Moreover, as shown by the observation that mesenchymal stem cells labelled with oligo-arginine-poly(ethylene glycol) (PEG)-coated $NaYF_4$:Yb,Er UCNPs maintain their stem cell potency,[48] the effect of UCNPs on cell behaviour is generally thought to be minimal. In spite of this, it is worth emphasizing that UCNPs are not necessarily toxicity-free. A previous study has reported that ligand-free lanthanide-doped nanoparticles can induce intracellular ATP deprivation in HeLa cells and can result in a significant decrease in cell viability.[49] Such UCNP-induced cell death is attributed to the interactions of the nanoparticles with the

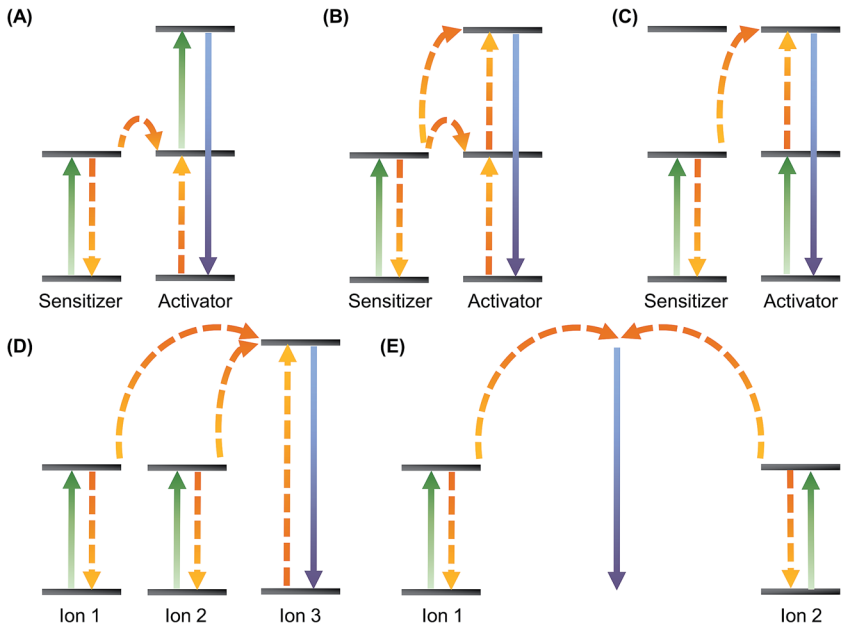

Fig. 1 General energy schemes related to different ETU processes in UCNPs: (A) energy-transfer followed by excited-state absorption; (B) successive energy transfer; (C) cross-relaxation upconversion; (D) cooperative sensitization; (E) cooperative luminescence. Green, orange and violet arrows represent the excitation light, energy transfer, and upconversion emission, respectively.

Table 2 A list of host-dopant systems commonly adopted for UCNP synthesis

Host lattice	Activator	Sensitizer	Excitation wavelength (nm)	Colour of light emission	Emission peak (nm)	Ref.
Lu_2O_3	Er, Tm	Yb	980	Blue, green, red	490, 540, 662	23
Y_2O_3	Er	Yb	980	Green, red	550, 660	25
	Ho	Yb	980	Green, red	543, 665	28
CaF_2	Er	Yb	980	Green, red	524, 654	29
LaF_3	Ho	Yb	980	Green, red	542, 645, 658	30
	Er	Yb	980	Green, red	520–545, 659	
	Tm	Yb	980	Blue	475	
$LuPO_4$	Tm	Yb	980	Blue, red	475, 649	31
$NaYF_4$	Ho	Yb	980	Green, red	542, 645–658	32
	Er	Yb	980	Green, red	510–540, 635–675	33–37
	Tm	Yb	980	Blue, red	450–457, 647	33
	Er, Tm	Yb	980	Blue, green, red	474–499, 525, 644–693	38

phosphate group of cellular ATP to cause apoptosis and autophagy.[49] Nevertheless, UCNPs have a comparatively high safety profile among commonly used luminescent nanoparticles.[40–47] Along with the ease of modulating their physicochemical properties *via* surface engineering, UCNPs turn out to be favourable building blocks for further development as multifunctional gene carriers.

3. Molecular design of UCNPs as gene carriers

A fundamental aspect of designing UCNP-based gene carriers is to determine the nanoparticle composition. When UCNPs are designed, dopant ions are often chosen by considering not only the spaced energy levels that govern photon absorption by the sensitizer, but also the energy transfer process between the sensitizer and the activator. Yb^{3+} has been widely adopted as a sensitizer, owing to its high absorption coefficient and upconversion efficiency.[50] In addition, the f–f transitions of many commonly used upconverting lanthanide ions (*e.g.*, Er^{3+} and Tm^{3+}) can be resonant with the $^2F_{7/2} \rightarrow {}^2F_{5/2}$ transition of Yb^{3+}. This further facilitates energy transfer from the sensitizer to the activator.[16] Regarding the selection of activators, common choices include Tm^{3+}, Ho^{3+} and Er^{3+},[16] although the use of other lanthanide ions (such as Tb^{3+}, Dy^{3+} and Pr^{3+}) has been occasionally reported in the literature.[51,52] To date, the most efficient UCNPs obtained have been those using Tm^{3+} and Er^{3+} as the activators. These ions have ladder-like energy levels,[16] and have relatively large energy gaps. These energy gaps can enhance luminescence emission, as suggested by the energy gap law:[53]

$$k_{nr} \propto \exp\left(-\beta \frac{\Delta E}{\hbar\omega_{max}}\right) \quad (1)$$

where k_{nr} represents the multiphonon relaxation rate constant for 4f levels of a lanthanide ion; ΔE represents the energy gap between the populated level and the next lower-lying energy level of a lanthanide ion; β represents the empirical constant of the host; $\hbar\omega_{max}$ designates the highest-energy vibrational mode of the host lattice. The law reveals that the energy gap is negatively related to the multiphonon relaxation rate constant. In other words, the comparatively large energy gap possessed by Tm^{3+} and Er^{3+} can reduce the probability of having non-radiative transitions among different excited levels of ions, thereby increasing the efficiency of upconversion.

Apart from the nanoparticle composition, some other factors have to be considered so as to render the UCNPs applicable to gene delivery. For example, the nanoparticles should be biodegradable, biocompatible and non-toxic.[54–57] In addition, gene delivery mediated by UCNPs is a multi-stage process (Fig. 2). Contrary to the delivery of chemical drugs, in which the intervention will still be therapeutic even if the carrier fails to be internalized into cells but simply releases the payload outside, gene therapy is possible only when cellular internalization of the delivered gene is successful.[58–60] As far as cellular uptake is concerned, the size and zeta potential of the nanoparticles are two important determining factors. A small size can be achieved by surface passivation or functionalization to enhance the colloidal stability of UCNPs.[16,61] This is pivotal when the nanoparticles are to be used *in vivo*, in which salt ions in blood may

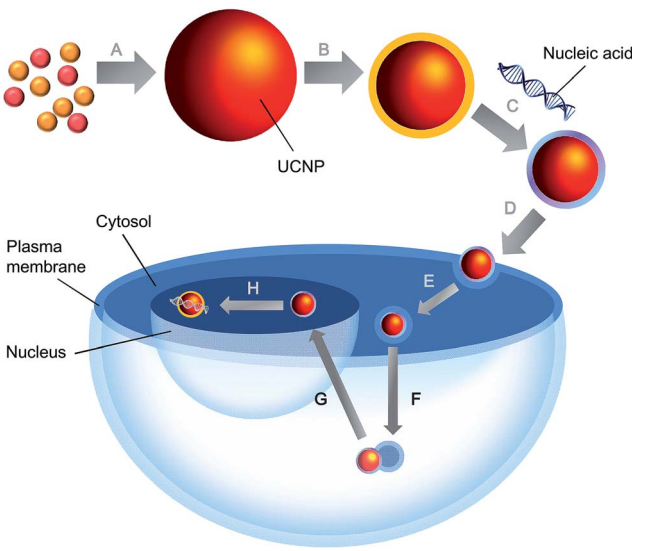

Fig. 2 Major processes of UCNP-based gene delivery: (A) synthesis of UCNPs; (B) surface modification; (C) gene loading; (D) cell attachment; (E) cellular internalization; (F) endolysosomal escape; (G) nuclear localization; (H) dissociation.

coordinate with the exposed lanthanide ions on the UCNP surface, causing nanoparticle aggregation. Regarding the zeta potential, it can be manipulated by incorporating a positively charged coating [*e.g.*, poly(ethylenimine) (PEI),[62] cationic lipids,[63] cetyl trimethylammonium bromide (CTAB),[64] dimethyldidodecylammonium bromide (DMAB),[64] and chitosan[65]] onto the nanoparticle surface. This facilitates the efficiency of the subsequent gene loading process, as well as the binding of UCNPs to the anionic plasma membrane. The cellular attachment and tissue specificity of the nanoparticles can be enhanced by conjugating ligands (such as folic acid,[66,67] galactose,[68] transferrin,[66,69] RGD peptide,[70,71] and antibodies[72,73]) to the nanoparticle surface for receptor-mediated endocytosis. The feasibility of this has been evidenced by an earlier study, in which folic acid and anti-Her2 antibody have been conjugated to silica-coated $NaYF_4$:Yb,Er UCNPs.[74] Compared to the unmodified counterparts, ligand-conjugated UCNPs exhibit higher transfection efficiency and gene silencing efficiency in SK-BR-3 cells, in which Her2 receptors are overexpressed.[74]

As UCNPs are mostly internalized *via* endocytosis, their ability to undergo endo-lysosomal escape (*e.g.*, by eliciting the proton sponge effect) may determine the ultimate success of the gene delivery process. In order for the delivery process to be therapeutic, plasmids also have to reach the nucleus whereas RNA molecules have to be released in the cytosol.[59] For the former, one strategy to facilitate the nuclear import of the delivered nucleic material is to incorporate the UCNP surface with nuclear localization signal (NLS) peptides (*e.g.*, PARP, M9-ScT conjugate, SV40 T antigen, Xenopus N1, adenovirus E1a, human c-myc, SV40 Vp3, and mouse FGF3),[75–78] which can localize the nanoparticles to the nucleus and allow them to be actively transported across the nuclear pore complex. But even with proper intracellular localization, careful manipulation of the UCNPs, in particular the surface properties and the buffering capacity of the polymer coating, is required because this may influence the process of gene release. Failure to dissociate the payload from the nanoparticles at the right location can indeed influence the outcome deleteriously.

4. Fabrication of UCNP-based gene carriers

UCNP-based gene carriers can be constructed using various strategies. Co-precipitation is one of the simplest methods to generate UCNPs because it does not involve time-consuming procedures or severe reaction conditions.[79] By adding capping ligands into the solvent during the synthetic process, the growth of the nanoparticles can be controlled and the UCNPs can be stabilized. Examples of these capping ligands include polyvinylpyrrolidone (PVP), ethylenediaminetetraacetic acid (EDTA) and PEI.[37,80,81] In the case of $NaYF_4$:Yb,Er nanocrystals, the upconversion emission exhibited by those in the hexagonal phase is generally higher than that exhibited by the cubic-phase counterparts.[82] However, nanocrystals synthesized *via* co-precipitation are often in the cubic phase, and hence are not the most efficient upconverter.[83] To address this problem, calcinations at a high temperature can be applied to achieve the sharpened crystal structure or to mediate partial phase transfer to the hexagonal-phase nanocrystals.[37] Apart from $NaYF_4$:Yb,Er nanocrystals, other nanoparticles (*e.g.*, $LuPO_4$:Yb,Tm and $YbPO_4$:Er,Tm) have been successfully generated by co-precipitation, with subsequent heat treatment being applied to improve the upconversion efficiency.[84] Despite the wide application of co-precipitation in UCNP generation, particle aggregation may occur during the synthetic process, making precise control of the particle size difficult. As the size of the nanoparticles is an important parameter governing the efficiency of cellular internalization during the gene delivery process, the polydispersity of the generated nanocrystals is an issue to be tackled when the performance of a gene carrier is to be enhanced.

Another method of UCNP generation is thermal decomposition, in which solvents with a high boiling point (*e.g.*, octadecene, oleic acid and oleylamine) are often used to dissolve rare earth trifluoroacetate precursors, which are often thermolyzed at 300 °C or above.[85,86] Using this method, $LiYF_4$ and $KGdF_4$ UCNPs have been obtained.[87] Monodispersed hexagonal-phase $NaYF_4$:Yb,Er and $NaYF_4$:Yb,Tm nanoparticles with enhanced upconversion emission have been generated, too.[88] Notwithstanding this, due to the involvement of the use of expensive and air-sensitive metal precursors,[82] as well as the production of toxic by-products during the fabrication process,[85,88] the selection of this technique is not preferred sometimes. As an alternative to thermal decomposition, UCNPs can be synthesized *via* the sol–gel method, in which the metal precursors used are relatively cheap. This method has had a track record of applications in the fabrication of TiO_2:Er, ZrO_2:Er, $Lu_3Ga_5O_{12}$:Er, YVO_4:Yb,Er, and $BaTiO_3$:Er UCNPs.[89–93] Unfortunately, particle aggregation may occur when the nanoparticles generated by this method are dispersed in aqueous solutions. This limits the use of the nanoparticles in gene delivery, in which water is always the major medium through which gene carriers are delivered to target cells. Along with the occurrence of particle aggregation further induced by high-temperature calcinations, which is required to increase the crystalline phase purity so as to enhance luminescence emission, the sol–gel approach might not be the most suitable method for generation of UCNP-based gene vectors.

Apart from those mentioned above, UCNPs can be generated by the combustion method[94,95] or by the hydro(solvo)thermal process.[96–98] Contrary to the former in which proper control of the particle size is challenging and the crystalline phase purity is generally low, the latter can generate high-quality UCNPs upon proper control of the process parameters (*e.g.*, pH, reaction time, reaction temperature, and the type of precursors).[96–98] In an earlier study, α- and β-phase $NaYF_4$:Yb,Er UCNPs with well-controlled size and morphology have been generated using the hydrothermal method, with EDTA and citrate being used as the capping ligands.[99] The size of the particles has been shown to be controllable by manipulating the nucleation rate, which, in turn, can be adjusted by modulating the reactant concentration or by changing the type of ligands adopted.[99] In addition, by modifying the reaction time as well as the reactant

concentration, phase transformation for the nanoparticles can be achieved.[99] This phenomenon can be exploited to control the morphology of the generated UCNPs. Lately, polymer-coated UCNPs with high aqueous solubility have been generated based on the hydro(solvo)thermal mechanism.[100] The high hydrophilicity has rendered the UCNPs favourable to be utilized in biological applications. Due to the ease of control of the properties (*e.g.*, size, structure, and morphology) of the generated nanoparticles, along with the possibility of synthesizing the nanoparticles in a "one-pot" process,[81,92,101] the hydro(solvo)thermal method is and will continue to be one of the most favourable and convenient synthetic routes, in the practical sense, to UCNP-based gene carriers.

5. Surface modification of UCNPs for gene delivery

Surface modification can be adopted to optimize the biological performance of UCNP-based gene carriers (Fig. 3). The roles played by surface modification can be two-fold. One is to improve the gene loading efficiency, and the other is to optimize the physicochemical properties of the nanoparticles for better biological performance. Each of these roles will be discussed in more detail in this section.

5.1 Enhancement of the gene loading process

Upon fabrication of the nanoparticles, usually surface modification with cationic moieties will be exercised to render the nanoparticles applicable to gene loading. Polyelectrolyte complexation between nucleic acids and the cationic moieties on the nanoparticle surface is hitherto the most fundamental gene loading mechanism. In an earlier study, the surface of silica-coated $NaYF_4$:Yb,Er UCNPs has been modified with amine groups using *N*-[3-(trimethoxysilyl)propyl]ethylenediamine (AEAPTMS), and as shown by the gel retardation assay, the modified UCNPs can complex with RNA molecules *via* electrostatic interactions between the positively charged amine groups and the negatively charged nucleic acid material.[74]

Surface modification of UCNPs can also be achieved by direct incorporation with polycations. One representative polycation used in this aspect is PEI, which is a cationic aziridine polymer with high proton buffering capacity over a wide range of pH values.[57,102] PEI has been extensively adopted for non-viral delivery of nucleic materials (including plasmids,[103] oligonucleotides[104] and ribozymes[105]) in reagent-consuming animal studies. Its transfection efficiency can be optimized by modulating the physical–chemical features (*e.g.*, charge density, degree of branching, and molecular weight) of the PEI molecules,[106–108] and by optimizing the transfection conditions (*e.g.*, polyplex concentration and incubation time)[109] and polyplex properties (*e.g.*, zeta potential and particle size).[109] In a previous study, gadolinium (Gd^{3+})-doped UCNPs have been modified first by covalently conjugating PEG onto the nanoparticle surface, followed by deposition of PEI coatings using the layer-by-layer assembly technique.[110] The PEI-coated UCNPs have not only been shown to be more effective in transfection than the uncoated counterparts,[110] but have also been reported to exhibit high gene delivery efficiency in the serum-containing environment, in which native PEI has experienced a significant drop in the efficiency of transfection.[110] The nanoparticles have shown potential to be further developed into a gene carrier for biological use, in particular when parental administration of the therapeutic gene is required. Apart from PEI, other polycations have been adopted in the literature to coat UCNPs for enhancing the process of gene loading. For instance, PEG–poly(lactic-*co*-glycolic acid) (PEG–PLGA), along with a positively charged amphiphilic polymer synthesized by aminolyzing polysuccinimide (PSI) with *N*-(3-aminopropyl)imidazole (NAPI) and oleylamine, has been utilized to coat hydrophobic $NaYF_4$:Yb,Er UCNPs.[111] Owing to the presence of the cationic coating, genes can effectively adsorb onto the UCNP surface,[111] rendering the nanoparticles applicable as gene vehicles.

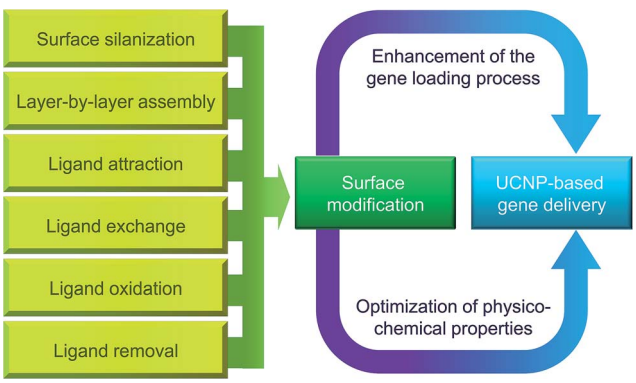

Fig. 3 Surface modification of UCNPs for gene delivery.

5.2 Optimization of physicochemical properties

Not only effective drug loading but also high aqueous solubility is vital to the proper functioning of UCNPs when the nanoparticles are used as gene carriers. Yet a majority of lanthanide-doped UCNPs are poorly soluble in the aqueous environment. In recent years, several surface functionalization strategies have been put forward to increase the hydrophilicity of UCNPs.[16] One method is surface silanization,[112] whose applications in surface modification have been rapidly growing due to the availability of well-established routes to silica-coated nanoparticles and the applicability of silica-coating to both hydrophobic and hydrophilic surfaces.[113,114] The feasibility of applying surface silanization to surface engineering of UCNPs has been demonstrated in a previous study, in which the affinity of PVP with silica has been exploited to coat PVP-stabilized $NaYF_4$:Yb,Er nanocrystals with a uniform silica shell having a thickness of approximately 9 mm.[115] A similar approach has been used by Li and Zhang.[112] They have produced water-soluble silica-coated PVP-stabilized $NaYF_4$:Yb,Er nanocrystals whose shell thickness can be tuned by changing the concentration of tetraethoxysilane (TEOS), which is a precursor during the process of silica formation. All of these have evidenced the practicality of silica-coating in surface modification of UCNPs. Lately, Wang and co-workers

have reported the fabrication of fluorescent silica-coated mesoporous microcarriers.[116] The microcarriers show extended residence time of up to 3 days in the gastrointestinal tract, releasing more than 60% of their content. They can also emit in the near-infrared window of 1000–1400 nm,[116] thereby enabling real-time tracking of the microcarrier fate as well as allowing for semi-quantitative monitoring of the content of drug release *in vivo*.[116] Although at the moment the nanocarriers have been evaluated only for drug delivery, this study has offered insights into possible strategies for monitoring the kinetics and dynamics of a delivered agent after administration to a living body. Along with the good biocompatibility of silicon, surface silanization may turn out to be promising for engineering the surface properties of UCNP-based gene carriers for theranostic applications in the future.

Other than surface silanization, surface engineering of UCNPs can be performed using non-silane reagents *via* diverse mechanisms, such as layer-by-layer assembly,[34] ligand attraction,[117] ligand exchange,[88] ligand removal[118] and ligand oxidation.[119] For instance, by taking advantage of electrostatic attraction, Hilderbrand *et al.* have coated UCNPs with a layer of polyacrylic acid (PAA) *via* electrostatic layer-by-layer assembly,[120] during which the carboxyl groups of PAA have been linked covalently with amino-modified PEG. *Via* the process of ligand exchange, an earlier study has also replaced the oleylamine ligands, which have been used to stabilize $NaYF_4$:Yb,Er nanoparticles, with bifunctional organic molecules to render the nanoparticle surface hydrophilic.[88] More recently, based on the phenomenon that PEI and PAA exhibit higher binding affinity than PVP towards lanthanide ions, PEI- and PAA-coated $NaYF_4$:Yb,Er UCNPs have been generated from PVP-stabilized nanoparticles.[121] The UCNPs show good dispersibility in aqueous media after the ligand exchange process.[121] More details of different surface modification strategies to enhance the aqueous solubility of UCNPs are presented in Table 3.

Surface modification can not only improve the particle hydrophilicity but can also modulate the physiochemical properties of UCNPs, thereby enhancing the efficiency of gene delivery. This has been revealed by multiphoton confocal microscopy and inductively coupled plasma mass spectrometry (ICP-MS) measurements, in which the PEI-coated UCNPs have been found to display greater efficiency in cellular internalization as compared to their counterparts having neutral or negative surface charges.[121] In addition to PEI, PEG is another polymer widely used as a surface modifier due to its capacity of enhancing the aqueous solubility of various nanoparticulate gene delivery systems[122] and of reducing particle aggregation.[123] Attributed to the hydrophilic nature of PEG and the brush-type polymer crowding,[124] PEGylated particles are usually less prone to opsonization and reticuloendothelial system (RES) uptake, and hence having the blood circulation time lengthened.[124,125] Despite this, every coin has two sides. As hinted at by an earlier study, polyplexes that have undergone PEGylation display premature vector unpackaging in blood, causing a decline in the gene delivery efficiency to the liver.[126] Similar problems have been delineated by Mishra *et al.*,[127] who have found that the cellular uptake and intracellular trafficking of polyplexes are impeded after PEGylation, even though the salt stability of the polyplexes is enhanced. Taking all these into account, to maximize the positive effect of PEGylation in the molecular design of UCNP-based gene carriers, structural properties (*e.g.*, density, conformation, molecular weight, and flexibility) of the PEG moiety and the degree of PEG grafting have to be carefully considered before PEGylation is executed. In addition, acid-labile linkages (*e.g.*, vinyl ether,[128] acetals,[129,130] and hydrazones[131]) can be used to link the PEG shield to the UCNP surface. The linkage can then be hydrolyzed in the acidic milieu of the endosomal compartment, leading to shielding destabilization and therefore mitigating the possible drawback of PEGylation to endolysosomal escape.[132]

6. Recent advances in UCNP-based gene transfer

With advances in the molecular design of UCNPs and the continuous development of technologies for materials fabrication, over the years copious UCNP-based carriers have been developed for delivery of nucleic acid materials. Based on the nature of the materials to be delivered, these carriers can be categorized into two types. One is for DNA delivery, and the other is for RNA delivery.

6.1 UCNP-based DNA delivery

As far as UCNP-based gene transfer is concerned, most of the efforts in the literature have been devoted to DNA delivery, whose practical potential in biomedicine has been evidenced in a pre-clinical trial, in which aminosilane-modified $NaYF_4$:Yb,Er UCNPs have been exploited as carriers for DNA vaccination to combat foot-and-mouth disease (FMD).[133] The UCNPs can complex with the plasmid pcDNA3.1/VP1-GFP *via* electrostatic interactions, and protect the plasmid from DNase I degradation.[133] As revealed by *in vitro* studies, the transfection efficiency of the nanoparticles is comparable to lipofectamine, but with lower cytotoxicity.[133] Upon intramuscular injection of the UCNP/DNA complex to guinea pigs, induction of the humoral and cellular immune responses has been achieved.[133] The serum levels of anti-FMDV specific antibodies and neutralizing antibodies, as well as the proliferation of T-lymphocytes, have also been found to be enhanced.[133] As confirmed by the challenge test, the guinea pigs vaccinated with the UCNP/DNA complex have been fully protected from attack by the FMD virus.[133] This study has pointed to the possible use of UCNP-based gene carriers in preventive medicine. Despite this, the unique optical properties of UCNPs have not been exploited during the design of the DNA vaccine carrier. Making use of those properties in the delivery system for additional capacity (*e.g.*, photo-triggered release of the delivered plasmid during the vaccination process) can be the next rewarding step to pursue to escalate the application potential of the carrier in the clinical context. In fact, UCNPs can play at least two roles when they are incorporated into the design of a gene delivery system: (1) imaging-monitored gene delivery and therapy, and (2) temporal–spatial

Table 3 Common strategies to modify the UCNP surface to enhance hydrophilicity

Strategy	Basic principle	Example of application	Ref.
Layer-by-layer assembly	Polyions with opposite charges are deposited onto the UCNP surface layer by layer *via* electrostatic absorption	Water-soluble $NaYF_4$:Yb,Er UCNPs have been generated by sequential adsorption of poly(allylamine hydrochloride) (PAH) and poly(sodium 4-styrenesulfonate) (PSS) onto the nanoparticle surface	34
Ligand exchange	Bifunctional molecules are used to displace the ligands originally coordinating to the UCNP surface	Bifunctional organic molecules (PEG 600 diacid) have been adopted to replace the oleylamine ligands originally used to stabilize the $NaYF_4$:Yb,Er nanoparticles. The nanoparticles have shown good aqueous solubility after the ligand exchange process	88
Surface silanization	By hydrolysis and condensation of siloxane monomers, an amorphous silica shell is grown on the UCNP surface	PVP-stabilized $NaYF_4$:Yb,Er UCNPs have been coated with silica by using tetraethoxysilane (TEOS) as a precursor. The silica-coated UCNPs can effectively disperse in aqueous solutions	112
Ligand attraction	An amphiphilic block copolymer is used to modify the UCNP surface by adsorbing onto the surface *via* hydrophobic interactions between the copolymer and the original surface ligand	Polyacrylic acid, which has been modified with 25% octylamine and 40% isopropylamine, has been used to coat $NaYF_4$:Yb,Er UCNPs which possess carboxyl groups on the surface. The coated nanoparticles can be readily dispersed in aqueous solutions	117
Ligand removal	Hydrophobic ligands coordinating to the UCNP surface are removed to increase the aqueous dispersibility of the nanoparticles	An acid treatment has been applied to remove the oleate ligands from the surface of oleate-capped $NaYF_4$:Er,Yb UCNPs. The ligand-free nanoparticles generated can effectively disperse in aqueous solutions	118
Ligand oxidation	The possible use of this strategy is limited to those UCNPs capped by ligands with unsaturated carbon–carbon bonds. To execute ligand oxidation, the Lemieux-von Rudloff reagent is often adopted to oxidize the carbon–carbon double bonds to pendant carboxylic functional groups	The Lemieux-von Rudloff reagent has been used to convert oleic acid-stabilized $NaYF_4$:Yb,Er UCNPs into water-dispersible nanoparticles	119

confinement of gene manipulation. Each of them will be discussed individually below.

6.1.1 Imaging-monitored gene delivery and therapy. One immediate advantage brought about by using UCNPs as gene carriers is the possibility to track the delivery process *via* luminescence-based imaging. Over the years, advances in luminescence-based imaging have substantially facilitated the unravelling of the mechanisms of disease progression[134] and guiding the development of treatment for diseases such as choroidal melanomas, whose microcirculation has been successfully imaged *in vivo* using an indocyanine green (ICG) fluorescent probe.[135] In UCNP-based gene delivery, the viability of integrating therapeutic and imaging functionalities into one single system has been shown by Bai *et al.*,[111] who have coated hydrophobic $NaYF_4$:Yb,Er UCNPs with PEG–PLGA and a positively charged PSI-based amphiphilic polymer.[111] Before the polymer coating process, the nanoparticles display high crystallinity with an average diameter of around 25 nm. Although there is an increase in the particle size after the coating process, the average size is still in the size range favourable for cellular internalization. Importantly, the coated nanoparticles exhibit good biocompatibility and reasonable gene delivery efficiency.[111] Photoluminescence measurements have indicated that the coated nanoparticles show emission bands at around 540 nm and 660 nm.[111] These two bands are assigned to $^4S_{3/2}$–$^4S_{15/2}$ and $^4F_{9/2}$–$^4I_{15/2}$ transitions, respectively. The red UCL emission given by the nanoparticles enables tracking of the *in vitro* delivery process without background fluorescence

interference.[111] This has rendered the UCNPs reported in the study applicable to imaging-guided therapy in the future.

Apart from luminescence-based imaging, UCNP-based gene carriers can be designed to mediate multimodal imaging. One example is provided by the case of PEI-coated $NaGdF_4$:Yb,Er UCNPs, which can not only deliver plasmids *in vitro* but can also serve as a contrast agent for UCL, magnetic resonance imaging (MRI) and computed tomography (CT) (Fig. 4).[136] Another example is given by He *et al.*,[110] who have modified the surface of Gd^{3+}-doped UCNPs with PEG and PEI for transfection. Results have confirmed that the nanoparticles can not only function as gene carriers, but also display emission peaks at around 540 and 660 nm.[110] Even though the intensity of luminescence emission drops to 80% when 2 layers of PEI are incorporated into the nanoparticle surface, the intensity of the emission is sufficient for luminescence-based imaging (Fig. 5).[110] Furthermore, as the nanoparticles are doped with Gd^{3+}, they can provide contrast in MRI. Compared to gadolinium-diethylenetriamine penta-acetic acid (Gd-DTPA), the nanoparticles with 2 layers of PEI have been found to have a much higher longitudinal relaxivity value.[110] Considering their versatile imaging capacity and transfection activity, upon further development and optimization, the nanoparticles have high potential to serve as a multifunctional carrier for future theranostic applications.

Despite the promising advances made in the field, owing to the low extinction coefficient and narrow band absorption of lanthanide ions,[137] the light absorbing ability of UCNPs is

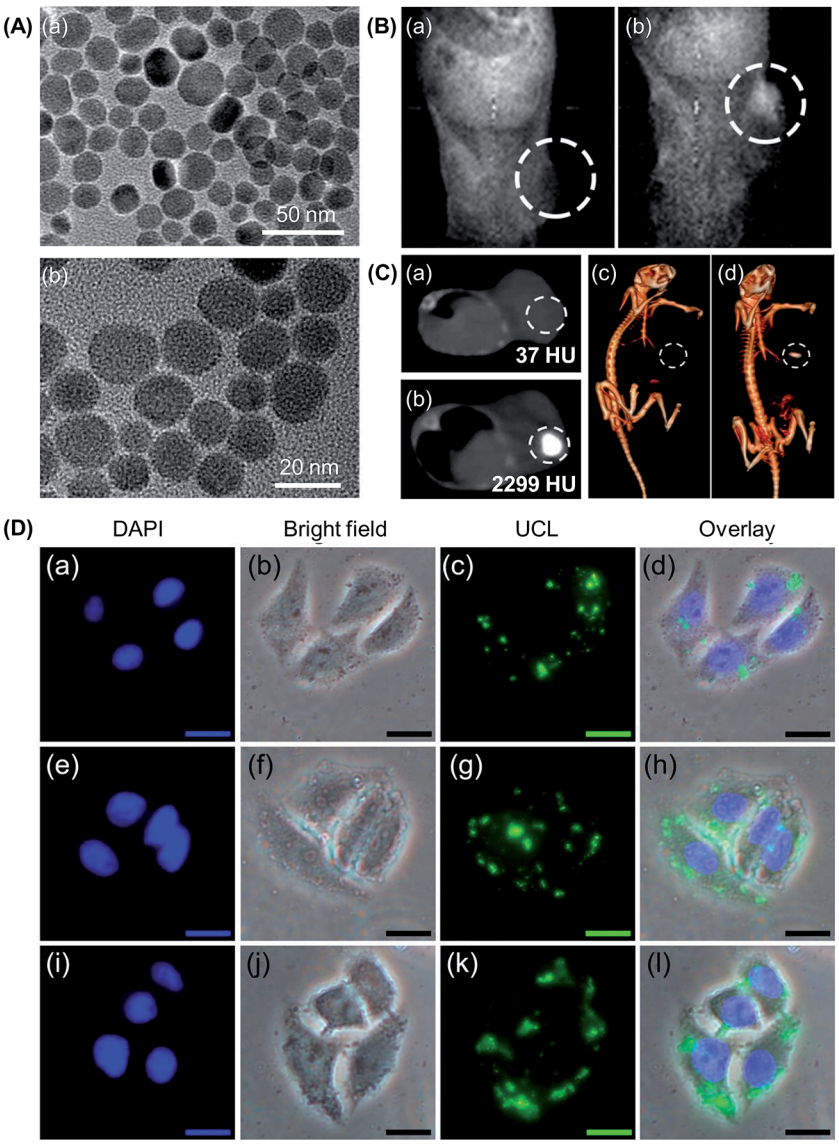

Fig. 4 (A) TEM images of (a) as-prepared UCNPs and (b) PEI-coated UCNPs. (B) *In vivo* T_1-weighted magnetic resonance images of a tumour-bearing mouse: (a) before and (b) after injection of the PEI-coated UCNPs *in situ*. (C) CT images of a tumour-bearing mouse: (a) before and (b) after injection of the PEI-coated UCNPs *in situ*, and (c and d) the corresponding 3D renderings of the CT images. (D) Inverted fluorescence microscopy images of HeLa cells incubated with the PEI-coated UCNPs for (a–d) 0.5 h, (e–h) 1 h, and (i–l) 3 h. The scale bar represents 20 μm (adapted from ref. 136 with permission from the American Chemical Society).

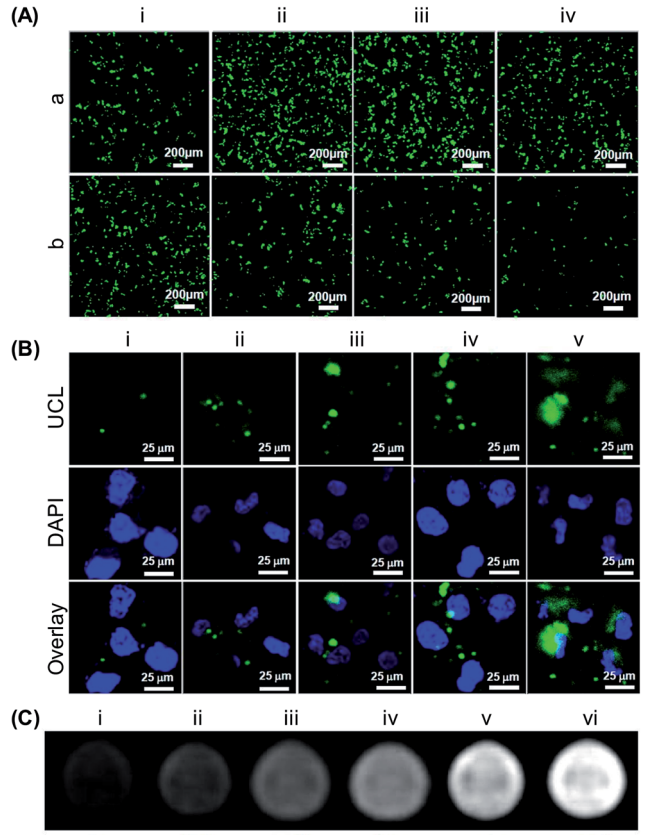

Fig. 5 (A) Confocal fluorescence images of HeLa cells transfected using (a) PEI or (b) UCNP-PEG@2×PEI in the presence of various concentrations of fetal bovine serum: (i) 0%, (ii) 10%, (iii) 20% and (iv) 30%. The images were taken 48 h after the initiation of transfection. (B) Confocal UCL/fluorescence images of HeLa cells after 4 hours of incubation with various concentrations of UCNP-PEG@2×PEI: (i) 4.3 mg L^{-1}, (ii) 8.7 mg L^{-1}, (iii) 17.3 mg L^{-1}, (iv) 34.7 mg L^{-1}, and (v) 69.4 mg L^{-1}. (C) T_1-weighted MRI images of HeLa cells after 4 hours of incubation with various concentrations of UCNP-PEG@2×PEI: (i) 0 mg L^{-1}, (ii) 4.3 mg L^{-1}, (iii) 8.7 mg L^{-1}, (iv) 17.3 mg L^{-1}, (v) 34.7 mg L^{-1}, and (vi) 69.4 mg L^{-1}. The cells were suspended in a 1% agarose gel for MRI (adapted from ref. 110 with permission from the American Chemical Society).

generally limited. This restrains the wide application of many of the reported UCNP-based gene carriers in imaging procedures. This situation is worsened by the fact that those carriers are in the nano-size range. The surface-to-volume ratio is, therefore, very high. This makes the emission efficiency of those carriers highly sensitive to surface-related deactivations. These deactivations can not only occur *via* direct deactivations, by neighbouring quenching centres, of the photoexcited dopants located on or around the UCNP surface, but can also happen if the energy possessed by the photoexcited dopants located in the centre of the nanoparticle randomly migrates to the dopants on or around the carrier surface or directly to the surface quenching sites. To solve this problem, one strategy is to take advantage of the antenna effect from other species with strong light-absorbing ability (*e.g.*, plasmons, QDs or organic dyes) to compensate for the low extinction coefficient resulting from 4f–4f optical transitions in lanthanide ions. Another strategy is to suppress the surface-related quenching mechanisms by incorporating the UCNPs with a core–shell structure, in which the host material of the shell shows a low lattice mismatch with the core material. To fabricate UCNPs with the core–shell architecture, shell layers are usually deposited onto core nanocrystals *via* epitaxy.

Epitaxial shells can be grown through chemical reactions similar to those adopted to generate the core particles, except that the process of crystal growth occurs on the core surface rather than in the liquid phase. To achieve epitaxial shell coating, one method is to use the heat-up strategy, which allows for the generation of UCNPs with a multi-shelled structure by either repeating the same synthetic protocol multiple times, or by arbitrarily combining dissimilar synthetic approaches for deposition of shells with different properties onto the same core crystal.[138] The viability of this strategy to enhance photoluminescence has been demonstrated by Zhang *et al.*,[139] who have heated $NaYF_4$:Yb,Er nanocrystals in an oleic acid/1-octadecene solution containing precursors for the formation of the hexagonal $NaGdF_4$ shell. Another strategy for epitaxial growth is the hot-injection method, in which a sequence of shell precursors is injected into a host reaction for the one-pot synthesis of multi-shelled nanoparticles.[117] The use of this method was first reported in the early 2000's when $NaYF_4$:Yb,Er@$NaYF_4$ core–shell UCNPs were synthesized by first heating related rare earth trifluoroacetates in oleylamine for the growth of the $NaYF_4$:Yb,Er core nanoparticles, followed by the injection of an oleylamine solution containing the shell precursors to achieve epitaxial deposition of the undoped $NaYF_4$ shell layer.[117] Using a similar approach, the synthesis of few other core–shell UCNPs (*e.g.*, $NaGdF_4$@$NaGdF_4$ and $LiLuF_4$@LiLuF4) has been reported in the literature.[140–142]

Apart from the aforementioned methods of epitaxial growth, deposition of the shell layer can be exercised in a non-epitaxial manner, in which the shell layer can be immobilized on the surface of pre-synthesized UCNPs either by means of chemical bonding or through surface polymerization.[143,144] Such methods have been employed for fabricating silica-coated $NaYF_4$:Yb,Er UCNPs[144] and $NaYF_4$:Yb,Tm UCNPs with tuneable surface coverage of gold nanoparticles.[145] With the incorporation of the multi-shelled nanostructure, the emission efficiency of UCNPs has been shown to be enhanced in several reports. For instance, after coating with an undoped $NaYF_4$ shell, UCL emission from $NaYF_4$:Yb,Er and $NaYF_4$:Yb,Tm UCNPs has been found to be remarkably enhanced.[117] $NaYF_4$:Yb,Er UCNPs with a hexagonal $NaGdF_4$ shell have also been reported to give more intense overall emission than the uncoated counterparts, owing to the passivation of surface defects of the nanocrystals by shell deposition.[139] All of these have evidenced the effectiveness of the core–shell nanostructure in enhancing the emission intensity of UCNPs and in strengthening the capacity of the nanoparticles to mediate imaging-monitored gene delivery and therapy in practice.

6.1.2 Temporal–spatial confinement of gene manipulation. To achieve target-specific gene delivery, ligand conjugation to the carrier surface is a prevailing strategy; however, controlled release of nucleic acids may represent a new

direction. The latter can be achieved using photoactivatable molecules that release payloads at specific sites upon UV irradiation.[146] The clinical application of this strategy has unfortunately been impeded by the toxicity and low tissue penetration power of UV light. This problem may be solved using UCNPs, which can convert near-infrared (NIR) or visible light to UV *in situ* to regulate the process of gene manipulation. The possible use of UCNPs to precisely control gene expression has recently been demonstrated in tumour cells that have been transplanted into adult zebrafish.[147] Similar success has also been reported on silica-coated $NaYF_4$:Yb,Tm nanocrystals,[148] in which the NIR-to-UV upconversion process has been exploited to silence the expression of target genes in a temporally and spatially specific manner. Such ability to manipulate gene expression has provided practical implications not only for treatment development but also for fundamental research on signal transduction. All of these are beyond the reach of conventional gene delivery methods.

As a matter of fact, while using UCNPs to control the location of gene manipulation is relatively new; similar concepts have already been used extensively in drug delivery research, in which UV light has been applied to manipulate the timing, dosage, and location of drug release.[149–152] The process of photo-triggered drug release is mediated by molecule excitation upon photon absorption and by the subsequent relaxation process, which is achieved *via* radiative and non-radiative pathways. In the radiative process, energy is usually emitted in the form of fluorescence when the molecule in the excited state returns to the ground state; whereas in the non-radiative scenario, multiple pathways can be involved. One pathway is internal conversion, in which energy is released in the form of heat from an excited molecule. Another pathway is intersystem crossing, which involves the conversion of the singlet state of an excited molecule into a triplet state without emission of photons. In addition to these, excited molecules may undergo photochemical reactions (*e.g.*, photocleavage, Wolff rearrangement, photoisomerization, and photocrosslinking) and experience non-radiative decay. Incorporation of these reactions into the molecular design of UCNP-based gene carriers is scant at the moment, but these reactions have already been well-adopted to control the delivery of chemical drugs.[146,149,153,154] A good example has been given by Matyjaszewski and co-workers, who have synthesized a block copolymer having poly(ethylene oxide) (PEO) as the hydrophilic segment and poly(spiropyran methacrylate) as the hydrophobic part.[155] In an aqueous medium, the copolymer forms micelles with a core–shell structure. These micelles are disrupted upon UV irradiation, which causes the spiropyran unit to undergo a reversible isomerization between hydrophobic spiropyran (SP) and hydrophilic merocyanine (ME), leading to the release of the encapsulated agent. Upon irradiation with visible light, photochemical reversion from ME to SP occurs, and the disrupted micelles are reformed. More examples demonstrating the possible use of photochemical reactions in controlling payload release are provided in Table 4.[156–162] In view of the similar nature between drug delivery and gene delivery, translating these strategies into the molecular design of UCNP-based gene carriers is not only theoretically feasible but may also enable more precise control of UCNP-mediated gene manipulation in the future.

6.2 UCNP-based RNA delivery

If an UCNP-based gene carrier can load DNA *via* electrostatic interactions, the same carrier should be applicable to complex with RNA for delivery purposes, due to the similarity of the electrostatic properties between DNA and RNA molecules. Nevertheless, RNA shows extra vulnerability to enzymatic degradation, and proper protection of the RNA molecules during the delivery process is vital. An example of UCNP-mediated RNA transfer is presented by an earlier study, in which UCNPs have been prepared by first encapsulating Yb^{3+}/Tm^{3+} co-doped nanocrystals in a silica shell with surface amine groups, followed by surface functionalization with cationic photocaged linkers to make siRNA loading feasible (Fig. 6).[163] Upon NIR irradiation, the photocaged linker on the UCNP surface is cleaved by upconverted UV light.[163] This initiates the release of siRNA molecules in a temporal–spatial manner. A similar approach has been adopted by Guo *et al.*,[148] who have used silica-coated $NaYF_4$:Yb,Tm UCNPs as a carrier of siRNA to act against the expression of survivin. Those siRNA molecules have been caged with 4,5-dimethoxy-2-nitroacetophenone (DMNPE) before RNA delivery, and are subsequently uncaged by UV emitted from the UCNP-based carrier upon NIR irradiation. The success of RNAi mediated by the carrier has been verified using immunoblot analysis, which has revealed a significant drop in survivin expression in murine bladder cancer cells (MB49 cell line).[148] With further optimization and characterization, the carrier may be further developed into a mediator of gene therapy in cancer treatment.

In addition to executing gene therapy alone, UCNP-based gene carriers may enable concomitant administration of multiple treatments. This has been exemplified by the positively charged polymer-coated $NaGdF_4$:Yb,Er UCNPs, which have been reported for execution of both photodynamic therapy (PDT) and gene therapy.[164] Results have shown that the carrier can be loaded with the photosensitizer, namely chlorin e6 (Ce6), and with siRNA molecules that can silence Plk1 expression (Fig. 7).[164] Upon excitation by NIR light at 980 nm, cancer cells are killed not only by cytotoxic singlet oxygen generated *via* resonance energy transfer from UCNPs to Ce6, but also by the anti-tumour activity of the siRNA molecules.[164] More recently, $NaLuF_4$:Gd,Yb,Er UCNPs have been synthesized using carboxyl-containing glutarate as surface ligands, followed by conjugation with cypate, which is a carbocyanine fluorophore with high photothermal conversion efficiency, through a hydrazide bond (Fig. 8A).[165] Due to the magnetic and optical properties of the generated UCNPs, the nanoparticles function as a dual-modality contrast agent for UCL and MRI to guide oncotherapy (Fig. 8B). Moreover, those UCNPs can effectively deliver siRNA molecules, which can act against heat shock protein 70, to cancer cells to enhance cell damage.[165] This damaging effect, along with photothermal ablation led by the conjugated cypate, has triggered significant antitumor activity (Fig. 8C).[165] Such

Table 4 Photochemical mechanisms commonly adopted in the molecular design of light-stimulated systems for delivery purposes[a]

Mechanism	Working principle	Photoresponsive groups	Use	Ref.
Photocleavage	Cleavage of a covalent bond is induced by light irradiation. This disrupts the integrity of the drug carrier, triggering the release of the drug molecules	NB group	Photodissociable polymeric micelles have been generated from a block co-polymer, in which poly(ethyleneoxide) is the hydrophilic block and poly(2-nitrobenzyl methacrylate) is the hydrophobic block. UV irradiation results in micelle disruption and hence the release of the loaded compound	156
			Polymeric vesicles have been generated from a diblock copolymer consisting of a hydrophilic PAA segment and a hydrophobic PMCL segment bridged by the NB linker. Upon UV irradiation, the vesicles disintegrate and the payload is released	157
Photoisomerization	Photo-induced changes in the molecular conformation (*e.g.*, *cis–trans* isomerization and reversible ring opening/closing reactions) of the photoisomerizable component of a drug delivery system may change the steric effects and other physical–chemical properties of that component. This leads to changes in the drug release properties of the system	Azobenzene, stilbene, spiropyran and dithienylethene	Photoswitchable nanoparticles have been generated from a spiropyran derivative and a lipid-PEG. Upon UV irradiation, the nanoparticles shrank, expelling drugs repeatedly	158
			TSUA molecules have bound to mesoporous silica nanoparticles, with β-cyclodextrin molecules being threaded onto the *trans*-TSUA stalks to seal the nanopores. The cyclodextrin rings are dissociated from the stalks upon UV irradiation, leading to the release of the cargo	159
Photocrosslinking	Polymerization induced by light may alter the structural integrity, and hence the drug release properties, of a system	Methacrylates and coumarin	Polymeric micelles have been generated from a diblock copolymer consisting of PEO as the hydrophilic block and poly(coumarin methacrylate) as the hydrophobic block. Interchain crosslinking and de-crosslinking have been induced by irradiation with light at different wavelengths. This results in changes in the rate of drug release from the micelles	160
			Photoresponsive mesoporous silica nanoparticles have been designed based on the principle of coumarin-based reversible photodimerization. The storage and release of guest molecules from the nanoparticles can be controlled by irradiating the system with light at different wavelengths	161

Table 4 (*Contd.*)

Mechanism	Working principle	Photoresponsive groups	Use	Ref.
Wolff rearrangement	The Wolff rearrangement of an α-diazocarbonyl yields a ketene, which can undergo further reactions to ultimately alter the drug release properties of a drug carrier	DNQ	Micelles have been fabricated from a PEG-lipid amphiphile, whose hydrophobic end has been incorporated with DNQ. Upon UV irradiation, DNQ converts to 3-indenecarboxylate, disrupting the integrity of the micelles and triggering the release of the payload	162

[a] Abbreviations: DNQ, 2-diazo-1,2-naphthoquinone; TSUA, 4-(3-triethoxysilylpropylureido)azobenzene; PAA, polyacrylic acid; PMCL, poly(methyl caprolactone); NB, *O*-nitrobenzyl.

a possibility of executing multiple therapies has illuminated the vast potential of UCNPs in treatment development.

7. UCNP-based gene delivery: limitations and possible solutions

Although, with the advances as presented above, the use of UCNPs as multifunctional gene carriers seems to be within reach, there are hurdles to overcome before clinical translation of innovations in the field can be in full gear. These hurdles are mainly related to either emission efficiency or physiological performance. These challenges as well as possible solutions will be discussed here for future research.

7.1 Manipulation of emission properties

Regarding the role played by photoluminescence emission from UCNPs in gene delivery applications as discussed in the preceding sections, the emission efficiency significantly determines the practicality of the nanoparticles in treatment. To date, the tunability of light emission has been attained by strategies such as controlling the dopant concentration, altering the host/activator combination, modulating the size- and shape-induced surface effects, designing the core–shell structures, or utilizing appropriate energy transfer or migration pathways. At this moment, tuning upconversion emission from UCNPs is often accompanied by a loss of the luminescence efficiency,[21] partly due to the deleterious cross relaxation events

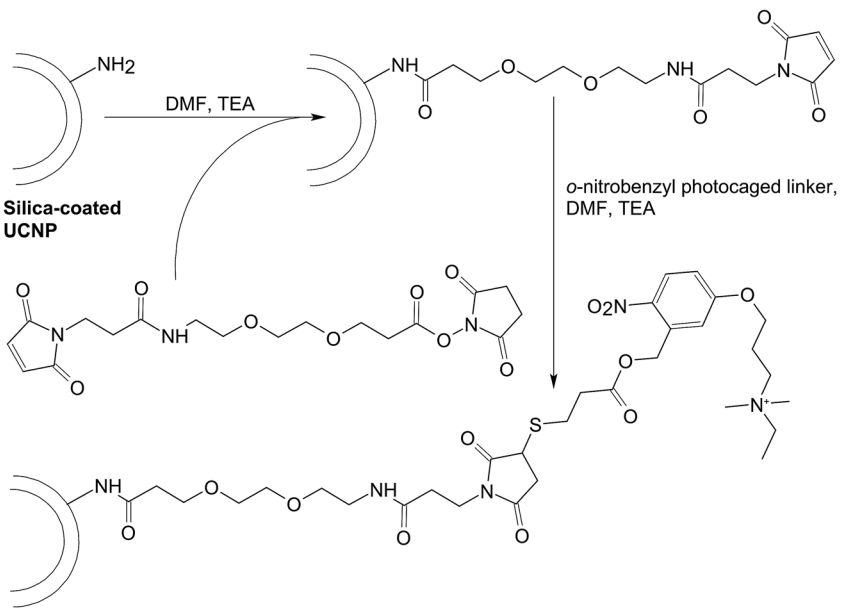

Fig. 6 The chemical routes for conjugating the cationic photocaged linker to the surface of the silica-coated UCNP. Abbreviations: DMF, dimethyl formamide; TEA, triethylamine.

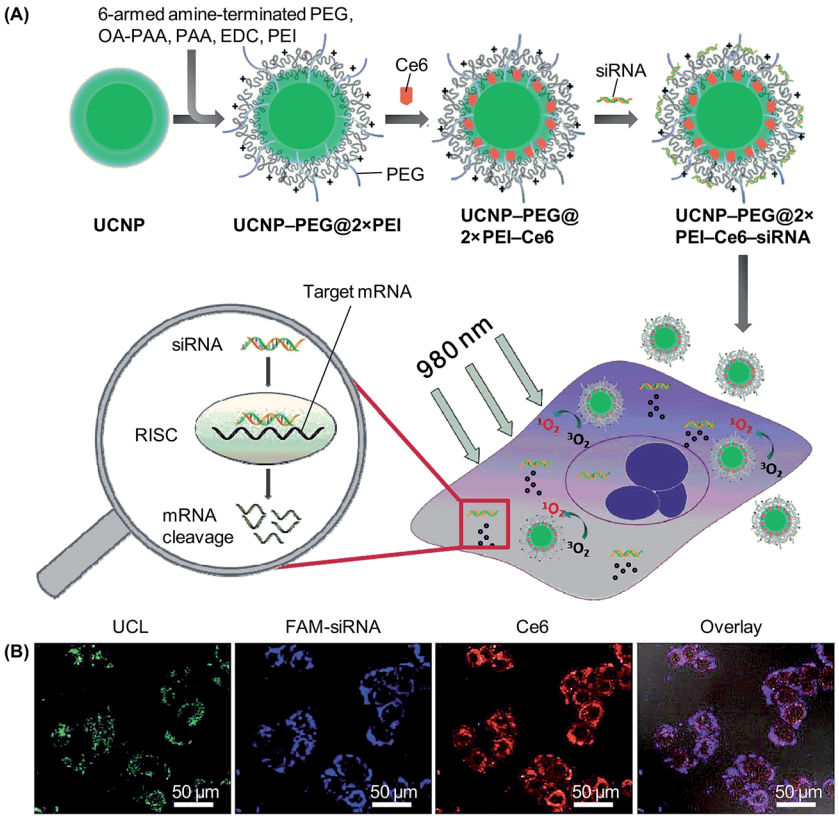

Fig. 7 (A) A schematic diagram depicting the functionalization of UCNPs, co-loading the nanoparticles with Ce6 and siRNA, and the implementation of the combined PDT and gene therapy mediated by the nanoparticles. Abbreviations: EDC, *N*-(3-dimethylaminopropyl-*N*′-ethylcarbodiimide)hydrochloride; OA, octylamine; PAA, poly(acrylic acid); PEG, poly(ethylene glycol); PEI, poly(ethylenimine); RISC, RNA-induced silencing complex. (B) Confocal microscopy images of HeLa cells after 4 hours of incubation with UCNP-PEG@2×PEI–Ce6–siRNA. The siRNA adopted was FAM-siRNA (adapted from ref. 164 with the permission of the Royal Society of Chemistry).

occurring between lanthanide ions. Yet, with an improvement in the efficiency of suppressing surface deactivations and in addressing different aspects of the colour tuning process, a new dimension brought to light emission tuning will be around the corner.

To induce luminescence emission from UCNPs, light at 980 nm is commonly used at the moment because this wavelength matches with the absorption of the commonly used sensitizer (Yb^{3+}). Light at this wavelength, however, can be absorbed by water, generating heat that may damage biological tissues. The capacity of exciting UCNPs at more tissue-transparent wavelengths is thus highly desired. The feasibility of manipulating the excitation dynamics of UCNPs has been evidenced by the observation that the excitation wavelength of Yb^{3+}-containing UCNPs can be blue-shifted when Yb^{3+} is further sensitized by Nd^{3+} as the second sensitizer.[166,167] Such feasibility has been further supported by the development of $NaYF_4$:Nd,Yb@$NaYF_4$:Yb,Tm luminescent nanocrystals that can be excited at 745 nm and emit light at 803 nm for deep tissue imaging.[168] These nanocrystals can not only alleviate the occurrence of attenuation effects relating to visible emission, but can also mitigate the overheating constraint imposed by 980 nm irradiation. Lately, the success of tuning the excitation wavelength of UCNPs has also been achieved by Li *et al.*,[169] who have fabricated $NaGdF_4$:Yb,Er@$NaYF_4$:Yb@$NaGdF_4$:Yb,Nd@$NaYF_4$@$NaGdF_4$:Yb,Tm@$NaYF_4$ nanoparticles with the core-multishell architecture. Due to the absorption filtration effect of the $NaGdF_4$:Yb,Tm layer, the nanoparticles can give power-density independent orthogonal excitation-emission UCL. Intriguingly, by changing the thickness of the filtration layer, the relative intensities of Er^{3+}-dominated green emission and Tm^{3+}-prominent blue emission can be tuned. These works, along with the emergence of Er^{3+}-sensitized UCNPs which can be excited at multiple wavelengths for light emission,[39,170] have laid a foundation from which future efforts to manipulate the excitation wavelength of UCNPs to those transparent to tissues can be launched.

7.2 Optimization of the physiological performance

In addition to the limited luminescence efficiency, another challenge to be met is the poor biodegradability of UCNPs. Diagnostic agents injected into a human body, as required by the Food and Drug Administration (FDA), have to be completely eliminated in a reasonable timeframe.[171] This is to ensure that the area under the exposure curve can be minimized upon total body clearance. Unfortunately, UCNPs in general are not effective to be degraded and eliminated from the body. Earlier studies have reported that PAA-coated $NaYF_4$:Yb,Er

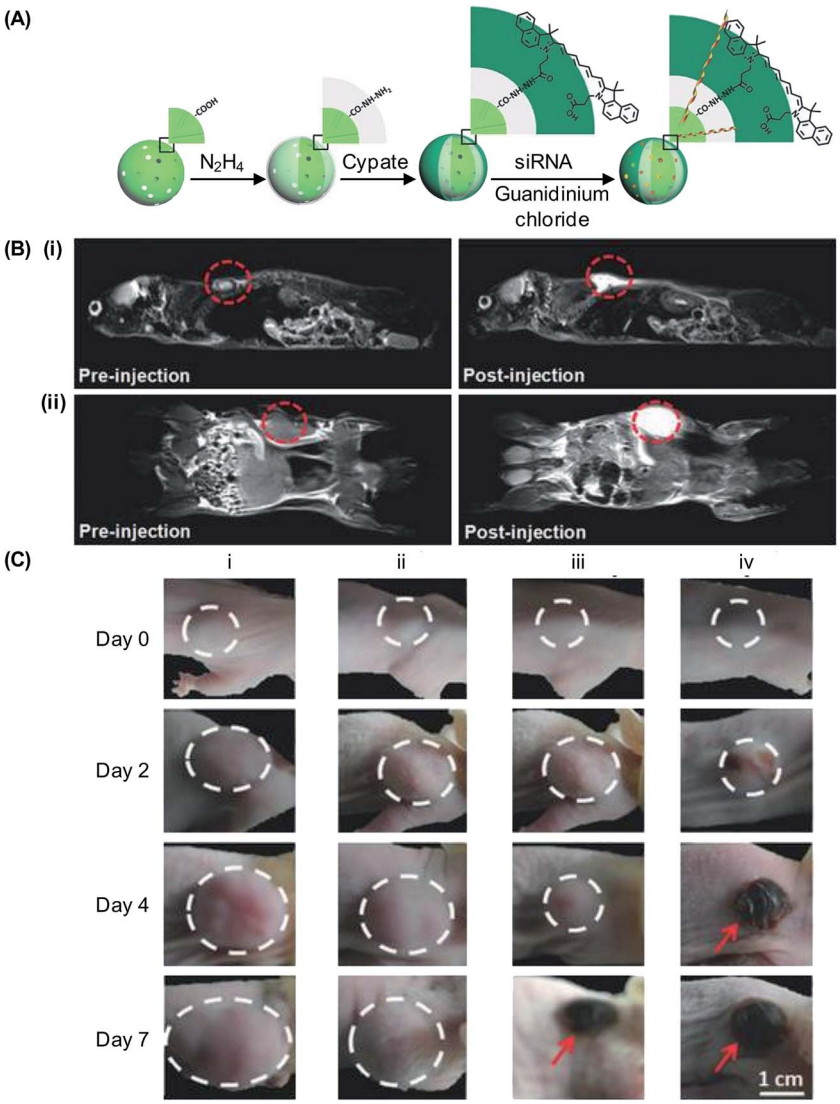

Fig. 8 (A) A schematic diagram showing the process of loading cypate and siRNA molecules into UCNPs. (B) (i) Sagittal and (ii) coronal plane MRI of a mouse before and after tail vein injection of the cypate-conjugated UCNPs (10 mg kg^{-1}). (C) Photographs depicting tumour development in mice treated with the (i) control (PBS), (ii) siRNA-loaded UCNPs, (iii) cypate-conjugated UCNPs, and (iv) siRNA-loaded cypate-conjugated UCNPs (adapted from ref. 165 with permission from John Wiley & Sons, Inc.).

nanoparticles with an average diameter of 11.5 nm take 115 days for complete excretion,[172] whereas those with a diameter of around 30 nm fail to be completely excreted even 90 days after *in vivo* administration.[173] To enhance excretion, the hydrodynamic size of UCNPs may need to be less than 10 nm.[21] Such hydrodynamic size, however, may not be the optimal diameter if gene transfer is involved. This is suggested by an earlier study in which PEI nanogels with mean diameters of 38, 75, 87, 121, 132 and 167 nm have been tested for transfection.[174] The highest efficiency has been shown to be achieved by particles that have mean diameters of 75 and 87 nm. This indicates that the optimal size for gene delivery may not coincide with the diameter of UCNPs that can be eliminated from the body most readily. The situation is more complicated when the UCNPs are used in preclinical and clinical studies, in which the size of the nanoparticles may affect the biodistribution pattern. In general, particles with a diameter smaller than 20–30 nm are more susceptible to renal excretion,[175,176] whereas those having a larger diameter may tend to accumulate in the bone marrow,[177] heart,[178] stomach,[179] kidney,[175,176] spleen[180] and liver.[181]

Based on what has been presented above, the size of the UCNP-based gene carrier is preferred to be small for facilitating elimination from the body upon administration, but from the gene delivery point of view, the optimal size may be defined in a totally different way. Solving such a discrepancy will be an obstacle to be tackled for clinical translation of works on UCNP-based gene delivery. Apart from size optimization, right now a disproportionate amount of resources has been directed towards characterization of the properties of UCNP-based carriers simply as emissive materials. Evaluation of the biocompatibility of the carriers at the organ and body levels is

lacking. To extend the use of the carriers from a laboratory context to clinical settings, additional efforts on evaluating the efficiency and long-term safety of the carriers will be the next stage to pursue.

8. Concluding remarks

Along with the advances in materials chemistry and fabrication,[182–187] there has been a clear trend in gene transfer to move from simply delivering nucleic acid materials to, more recently, systems into which multiple functions have been incorporated. In virtue of their unique optical properties, since the turn of the last century UCNPs have started to make remarkable strides towards gene delivery applications. Although at present the most compelling illustrations of the functional richness of UCNPs as gene carriers are still confined to imaging and light-controlled gene manipulation, with the increasing maturation of fabrication technologies, many of the practical problems (including the poor biodegradability and the low quantum yield) in UCNPs will become solvable someday. The use of UCNPs in gene delivery will ultimately be limited only by the imagination of the scientist.

Conflicts of interest

There are no conflicts to declare.

Acknowledgements

The authors would like to acknowledge Yau-Foon Tsui, Weijie Hu, Guoan Wang, Minjian Huang, Guoxing Deng, Fanyue Meng, Jinzheng Chen, Xiaoxin Cai and Jieling Li for helpful comments and suggestions during the writing of this manuscript. This work is supported by the HK Polytechnic University Area of Excellent Grants (1-ZVGG), Natural Science Foundation of Shenzhen University (2017092), and a grant from the Shenzhen Science and Technology Innovation Committee (JCYJ20170302144812937).

References

1 M. X. Yu, Q. Zhao, L. X. Shi, F. Y. Li, Z. G. Zhou, H. Yang, T. Yia and C. H. Huang, *Chem. Commun.*, 2008, **44**, 2115–2117.
2 J. S. Y. Lau, P. K. Lee, K. H. K. Tsang, C. H. C. Ng, Y. W. Lam, S. H. Cheng and K. K. W. Lo, *Inorg. Chem.*, 2009, **48**, 708–718.
3 Z. H. Luo, T. Fu, K. Chen, H. Y. Han and M. Q. Zou, *Microchim. Acta*, 2011, **175**, 55–61.
4 M. Martiez-Calvo, K. N. Orange, R. B. P. Elmes, B. L. Poulsen, D. C. Williams and T. Gunnlaugsson, *Nanoscale*, 2016, **8**, 563–574.
5 J. Tao, Q. Zeng and L. S. Wang, *Sens. Actuators, B*, 2016, **234**, 641–647.
6 Y. H. Zhang, Y. M. Zhang, Y. Yang, L. X. Chen and Y. Liu, *Chem. Commun.*, 2016, **52**, 6087–6090.
7 H. L. D. Lee, S. J. Lord, S. Iwanaga, K. Zhan, H. X. Xie, J. C. Williams, H. Wang, G. R. Bowman, E. D. Goley, L. Shapiro, R. J. Twieg, J. H. Rao and W. E. Moerner, *J. Am. Chem. Soc.*, 2010, **132**, 15099–15101.
8 I. Yang, J. W. Lee, S. Hwang, J. E. Lee, E. Lim, J. Lee, D. Hwang, C. H. Kim, Y. S. Keum and S. K. Kim, *J. Photochem. Photobiol., B*, 2017, **166**, 52–57.
9 C. Ma, T. Bian, S. Yang, C. Liu, T. Zhang, J. Yang, Y. Li, J. Li, R. Yang and W. Tan, *Anal. Chem.*, 2014, **86**, 6508–6515.
10 Q. A. Liu, C. Y. Li, T. S. Yang, T. Yi and F. Y. Li, *Chem. Commun.*, 2010, **46**, 5551–5553.
11 L. Yang, B. Shao, X. Zhang, Q. Cheng, T. Lin and E. Liu, *J. Biomater. Appl.*, 2016, **31**, 400–410.
12 Y. Xing, L. Li, X. Ai and L. Fu, *Int. J. Nanomed.*, 2016, **11**, 4327–4338.
13 U. Kostiv, I. Kotelnikov, V. Proks, M. Slouf, J. Kucka, H. Engstova, P. Jezek and D. Horak, *ACS Appl. Mater. Interfaces*, 2016, **8**, 20422–20431.
14 S. Y. Choi, S. H. Baek, S. J. Chang, Y. Song, R. Rafique, K. T. Lee and T. J. Park, *Biosens. Bioelectron.*, 2017, **15**, 267–273.
15 S. V. Eliseeva and J. C. Bunzli, *Chem. Soc. Rev.*, 2010, **39**, 189–227.
16 F. Wang and X. G. Liu, *Chem. Soc. Rev.*, 2009, **38**, 976–989.
17 F. Auzel, *Chem. Rev.*, 2004, **104**, 139–173.
18 P. D. Nguyen, S. J. Son and J. Min, *J. Nanosci. Nanotechnol.*, 2014, **14**, 157–174.
19 M. Gonzalez-Bejar, L. Frances-Soriano and J. Perez-Prieto, *Front. Bioeng. Biotechnol.*, 2016, **4**, 47.
20 X. Chen, D. Peng, Q. Ju and F. Wang, *Chem. Soc. Rev.*, 2015, **44**, 1318–1330.
21 G. Chen, H. Qiu, P. N. Prasad and X. Chen, *Chem. Rev.*, 2014, **114**, 5161–5214.
22 L. C. Ong, M. K. Gnanasammandhan, S. Nagarajan and Y. Zhang, *Luminescence*, 2010, **25**, 290–293.
23 J. Yang, C. M. Zhang, C. Peng, C. X. Li, L. L. Wang, R. T. Chai and J. Lin, *Chem.–Eur. J.*, 2009, **15**, 4649–4655.
24 S. K. Singh, A. K. Singh, D. Kumar, O. Prakash and S. B. Rai, *Appl. Phys. B: Lasers Opt.*, 2010, **98**, 173–179.
25 M. Kamimura, D. Miyamoto, Y. Saito, K. Soga and Y. Nagasaki, *Langmuir*, 2008, **24**, 8864–8870.
26 L. Sudheendra, V. Ortalan, S. Dey, N. D. Browning and I. M. Kennedy, *Chem. Mater.*, 2011, **23**, 2987–2993.
27 S. Liang, Y. Liu, Y. Tang, Y. Xie, H. Z. Sun, H. Zhang and B. Yang, *J. Nanomater.*, 2011, **2011**, 302364.
28 X. Qin, T. Yokomori and Y. G. Ju, *Appl. Phys. Lett.*, 2007, **90**, 073104.
29 G. F. Wang, Q. Peng and Y. D. Li, *J. Am. Chem. Soc.*, 2009, **131**, 14200–14201.
30 C. H. Liu and D. P. Chen, *J. Mater. Chem.*, 2007, **17**, 3875–3880.
31 S. Heer, O. Lehmann, M. Haase and H. U. Gudel, *Angew. Chem., Int. Ed.*, 2003, **42**, 3179–3182.
32 J. Shan, X. Qin, N. Yao and Y. Ju, *Nanotechnology*, 2007, **18**, 445607.
33 S. Heer, K. Kompe, H. U. Gudel and M. Haase, *Adv. Mater.*, 2004, **16**, 2102–2105.

34 L. Y. Wang, R. X. Yan, Z. Y. Hao, L. Wang, J. H. Zeng, J. Bao, X. Wang, Q. Peng and Y. D. Li, *Angew. Chem., Int. Ed.*, 2005, **44**, 6054–6057.
35 Z. Q. Li and Y. Zhang, *Nanotechnology*, 2008, **19**, 345606.
36 X. M. Liu, J. W. Zhao, Y. J. Sun, K. Song, Y. Yu, C. A. Du, X. G. Kong and H. Zhang, *Chem. Commun.*, 2009, 6628–6630.
37 G. S. Yi, H. C. Lu, S. Y. Zhao, G. Yue, W. J. Yang, D. P. Chen and L. H. Guo, *Nano Lett.*, 2004, **4**, 2191–2196.
38 F. Wang and X. G. Liu, *J. Am. Chem. Soc.*, 2008, **130**, 5642–5643.
39 N. J. Johnson, S. He, S. Diao, E. M. Chan, H. Dai and A. Almutairi, *J. Am. Chem. Soc.*, 2017, **139**, 3275–3282.
40 Z. Liu, Z. H. Li, J. H. Liu, S. Gu, Q. H. Yuan, J. S. Ren and X. G. Qu, *Biomaterials*, 2012, **33**, 6748–6757.
41 S. H. Gao, F. Y. Liu, B. T. Zhang, Y. J. Wang, H. M. Zhang and Z. X. Wang, *Chin. J. Anal. Chem.*, 2013, **41**, 811–816.
42 W. Zhang, B. Peng, F. Tian, W. Qin and X. Qian, *Anal. Chem.*, 2014, **86**, 482–489.
43 D. Yang, X. Kang, P. Ma, Y. Dai, Z. Hou, Z. Cheng, C. Li and J. Lin, *Biomaterials*, 2013, **34**, 1601–1612.
44 L. A. Cheng, K. Yang, S. A. Zhang, M. W. Shao, S. T. Lee and Z. A. Liu, *Nano Res.*, 2010, **3**, 722–732.
45 T. Cao, Y. Yang, Y. Sun, Y. Wu, Y. Gao, W. Feng and F. Li, *Biomaterials*, 2013, **34**, 7127–7134.
46 Y. Sun, M. Yu, S. Liang, Y. Zhang, C. Li, T. Mou, W. Yang, X. Zhang, B. Li, C. Huang and F. Li, *Biomaterials*, 2011, **32**, 2999–3007.
47 L. Q. Xiong, Z. G. Chen, M. X. Yu, F. Y. Li, C. Liu and C. H. Huang, *Biomaterials*, 2009, **30**, 5592–5600.
48 C. Wang, L. Cheng, H. Xu and Z. Liu, *Biomaterials*, 2012, **33**, 4872–4881.
49 J. Tian, X. Zeng, X. Xie, S. Han, O. W. Liew, Y. T. Chen, L. Wang and X. Liu, *J. Am. Chem. Soc.*, 2015, **137**, 6550–6558.
50 T. Soukka, T. Rantanen and K. Kuningas, *Ann. N. Y. Acad. Sci.*, 2008, **1130**, 188–200.
51 G. Lakshminarayana, J. R. Qiu, M. G. Brik and I. V. Kityk, *J. Phys. D: Appl. Phys.*, 2008, **41**, 175106.
52 H. J. Liang, G. Y. Chen, L. Li, Y. Liu, F. Qin and Z. G. Zhang, *Opt. Commun.*, 2009, **282**, 3028–3031.
53 J. M. F. Vandijk and M. F. H. Schuurmans, *J. Chem. Phys.*, 1983, **78**, 5317–5323.
54 W. F. Lai and M. C. Lin, *J. Controlled Release*, 2009, **134**, 158–168.
55 W. F. Lai, *Curr. Gene Ther.*, 2015, **15**, 55–63.
56 W. F. Lai, *Biomaterials*, 2014, **35**, 401–411.
57 W. F. Lai, *Expert Rev. Med. Devices*, 2011, **8**, 173–185.
58 W. F. Lai and Z. D. He, *J. Controlled Release*, 2016, **243**, 269–282.
59 W. F. Lai, *Ageing Res. Rev.*, 2013, **12**, 310–315.
60 W. F. Lai, *J. Biosci.*, 2011, **36**, 725–729.
61 S. Wilhelm, M. Kaiser, C. Wurth, J. Heiland, C. Carrillo-Carrion, V. Muhr, O. S. Wolfbeis, W. J. Parak, U. Resch-Genger and T. Hirsch, *Nanoscale*, 2015, **7**, 1403–1410.
62 J. Das, Y. J. Choi, H. Yasuda, J. W. Han, C. Park, H. Song, H. Bae and J. H. Kim, *Sci. Rep.*, 2016, **6**, 33784.
63 X. G. Pan, J. J. Guan, J. W. Yoo, A. J. Epstein, L. J. Lee and R. J. Lee, *Int. J. Pharm.*, 2008, **358**, 263–270.
64 F. Fay, D. J. Quinn, B. F. Gilmore, P. A. McCarron and C. J. Scott, *Biomaterials*, 2010, **31**, 4214–4222.
65 J. W. Wang, C. Y. Chen and Y. M. Kuo, *J. Appl. Polym. Sci.*, 2011, **121**, 3531–3540.
66 F. B. Jing, D. M. Li, W. Xu, Y. J. Liu, K. Wang and Z. G. Sui, *Pharm. Biol.*, 2014, **52**, 570–574.
67 W. F. Lai and M. C. Lin, *Curr. Gene Ther.*, 2015, **15**, 472–480.
68 Z. Y. Ong, C. Yang, S. J. Gao, X. Y. Ke, J. L. Hedrick and Y. Y. Yang, *Macromol. Rapid Commun.*, 2013, **34**, 1714–1720.
69 S. Somani, D. R. Blatchford, O. Millington, M. L. Stevenson and C. Dufes, *J. Controlled Release*, 2014, **188**, 78–86.
70 L. D. Kong, C. S. Alves, W. X. Hou, J. R. Qiu, H. Mohwald, H. Tomas and X. Y. Shi, *ACS Appl. Mater. Interfaces*, 2015, **7**, 4833–4843.
71 J. Park, K. Singha, S. Son, J. Kim, R. Namgung, C. O. Yun and W. J. Kim, *Cancer Gene Ther.*, 2012, **19**, 741–748.
72 S. Theoharis, U. Krueger, P. H. Tan, D. O. Haskard, M. Weber and A. J. T. George, *J. Immunol. Methods*, 2009, **343**, 79–90.
73 P. F. Pang, C. Wu, M. Shen, F. M. Gong, K. S. Zhu, Z. B. Jiang, S. H. Guan, H. Shan and X. T. Shuai, *PLoS One*, 2013, **8**, e76612.
74 S. Jiang, Y. Zhang, K. M. Lim, E. K. Sim and L. Ye, *Nanotechnology*, 2009, **20**, 155101.
75 M. Soniat and Y. M. Chook, *Biochem. J.*, 2015, **468**, 353–362.
76 L. M. McLane and A. H. Corbett, *IUBMB Life*, 2009, **61**, 697–706.
77 A. Lange, R. E. Mills, C. J. Lange, M. Stewart, S. E. Devine and A. H. Corbett, *J. Biol. Chem.*, 2007, **282**, 5101–5105.
78 R. Cartier and R. Reszka, *Gene Ther.*, 2002, **9**, 157–167.
79 H. Y. Du, W. H. Zhang and J. Y. Sun, *J. Alloys Compd.*, 2011, **509**, 3413–3418.
80 X. Y. Wu, H. J. Liu, J. Q. Liu, K. N. Haley, J. A. Treadway, J. P. Larson, N. F. Ge, F. Peale and M. P. Bruchez, *Nat. Biotechnol.*, 2003, **21**, 41–46.
81 F. Wang, D. K. Chatterjee, Z. Q. Li, Y. Zhang, X. P. Fan and M. Q. Wang, *Nanotechnology*, 2006, **17**, 5786–5791.
82 F. Wang, Y. Han, C. S. Lim, Y. H. Lu, J. Wang, J. Xu, H. Y. Chen, C. Zhang, M. H. Hong and X. G. Liu, *Nature*, 2010, **463**, 1061–1065.
83 M. Lin, Y. Zhao, S. Q. Wang, M. Liu, Z. F. Duan, Y. M. Chen, F. Li, F. Xu and T. J. Lu, *Biotechnol. Adv.*, 2012, **30**, 1551–1561.
84 Z. H. Xu, C. X. Li, P. P. Yang, Z. Y. Hou, C. M. Zhang and J. Lin, *Cryst. Growth Des.*, 2009, **9**, 4127–4135.
85 V. Mahalingam, R. Naccache, F. Vetrone and J. A. Capobianco, *Chem.–Eur. J.*, 2009, **15**, 9660–9663.
86 J. C. Boyer, F. Vetrone, L. A. Cuccia and J. A. Capobianco, *J. Am. Chem. Soc.*, 2006, **128**, 7444–7445.
87 Y. P. Du, Y. W. Zhang, L. D. Sun and C. H. Yan, *Dalton Trans.*, 2009, **40**, 8574–8581.
88 G. S. Yi and G. M. Chow, *Adv. Funct. Mater.*, 2006, **16**, 2324–2329.
89 Z. W. Quan, D. M. Yang, C. X. Li, D. Y. Kong, P. A. P. Yang, Z. Y. Cheng and J. Lin, *Langmuir*, 2009, **25**, 10259–10262.

90 A. Patra, C. S. Friend, R. Kapoor and P. N. Prasad, *J. Phys. Chem. B*, 2002, **106**, 1909–1912.
91 A. Patra, C. S. Friend, R. Kapoor and P. N. Prasad, *Chem. Mater.*, 2003, **15**, 3650–3655.
92 Y. X. Liu, W. A. Pisarski, S. J. Zeng, C. F. Xu and Q. B. Yang, *Opt. Express*, 2009, **17**, 9089–9098.
93 C. X. Li, Z. W. Quan, P. P. Yang, S. S. Huang, H. Z. Lian and J. Lin, *J. Phys. Chem. C*, 2008, **112**, 13395–13404.
94 N. Vu, T. K. Anh, G. C. Yi and W. Strek, *J. Lumin.*, 2007, **122**, 776–779.
95 J. N. Shan and Y. G. Ju, *Nanotechnology*, 2009, **20**, 275603.
96 F. Zhang, J. Li, J. Shan, L. Xu and D. Y. Zhao, *Chem.–Eur. J.*, 2009, **15**, 11010–11019.
97 Z. G. Yan and C. H. Yan, *J. Mater. Chem.*, 2008, **18**, 5046–5059.
98 W. B. Niu, S. L. Wu, S. F. Zhang, J. Li and L. A. Li, *Dalton Trans.*, 2011, **40**, 3305–3314.
99 Y. J. Sun, Y. Chen, L. J. Tian, Y. Yu, X. G. Kong, J. W. Zhao and H. Zhang, *Nanotechnology*, 2007, **18**, 275609.
100 M. Wang, C. C. Mi, J. L. Liu, X. L. Wu, Y. X. Zhang, W. Hou, F. Li and S. K. Xu, *J. Alloys Compd.*, 2009, **485**, L24–L27.
101 L. Y. Wang, Y. Zhang and Y. Y. Zhu, *Nano Res.*, 2010, **3**, 317–325.
102 M. Neu, D. Fischer and T. Kissel, *J. Gene Med.*, 2005, **7**, 992–1009.
103 Y. Liu, J. Nguyen, T. Steele, O. Merkel and T. Kissel, *Polymer*, 2009, **50**, 3895–3904.
104 P. Bandyopadhyay, X. M. Ma, C. Linehan-Stieers, B. T. Kren and C. J. Steer, *J. Biol. Chem.*, 1999, **274**, 10163–10172.
105 A. Aigner, D. Fischer, T. Merdan, C. Brus, T. Kissel and F. Czubayko, *Gene Ther.*, 2002, **9**, 1700–1707.
106 A. von Harpe, H. Petersen, Y. X. Li and T. Kissel, *J. Controlled Release*, 2000, **69**, 309–322.
107 K. Kunath, A. von Harpe, D. Fischer, H. Peterson, U. Bickel, K. Voigt and T. Kissel, *J. Controlled Release*, 2003, **89**, 113–125.
108 D. Fischer, T. Bieber, Y. X. Li, H. P. Elsasser and T. Kissel, *Pharm. Res.*, 1999, **16**, 1273–1279.
109 U. Lungwitz, M. Breunig, T. Blunk and A. Gopferich, *Eur. J. Pharm. Biopharm.*, 2005, **60**, 247–266.
110 L. He, L. Z. Feng, L. Cheng, Y. M. Liu, Z. W. Li, R. Peng, Y. G. Li, L. Guo and Z. Liu, *ACS Appl. Mater. Interfaces*, 2013, **5**, 10381–10388.
111 X. L. Bai, S. Y. Xu, J. L. Liu and L. Y. Wang, *Talanta*, 2016, **150**, 118–124.
112 Z. Q. Li and Y. Zhang, *Angew. Chem., Int. Ed.*, 2006, **45**, 7732–7735.
113 Y. Piao, A. Burns, J. Kim, U. Wiesner and T. Hyeon, *Adv. Funct. Mater.*, 2008, **18**, 3745–3758.
114 S. H. Liu and M. Y. Han, *Chem.–Asian J.*, 2010, **5**, 36–45.
115 N. J. J. Johnson, N. M. Sangeetha, J. C. Boyer and F. C. J. M. van Veggel, *Nanoscale*, 2010, **2**, 771–777.
116 R. Wang, L. Zhou, W. Wang, X. Li and F. Zhang, *Nat. Commun.*, 2017, **8**, 14702.
117 G. S. Yi and G. M. Chow, *Chem. Mater.*, 2007, **19**, 341–343.
118 N. Bogdan, F. Vetrone, G. A. Ozin and J. A. Capobianco, *Nano Lett.*, 2011, **11**, 835–840.
119 Z. G. Chen, H. L. Chen, H. Hu, M. X. Yu, F. Y. Li, Q. Zhang, Z. G. Zhou, T. Yi and C. H. Huang, *J. Am. Chem. Soc.*, 2008, **130**, 3023–3029.
120 S. A. Hilderbrand, F. W. Shao, C. Salthouse, U. Mahmood and R. Weissleder, *Chem. Commun.*, 2009, **45**, 4188–4190.
121 J. F. Jin, Y. J. Gu, C. W. Y. Man, J. P. Cheng, Z. H. Xu, Y. Zhang, H. S. Wang, V. H. Y. Lee, S. H. Cheng and W. T. Wong, *ACS Nano*, 2011, **5**, 7838–7847.
122 A. Kichler, M. Chillon, C. Leborgne, O. Danos and B. Frisch, *J. Controlled Release*, 2002, **81**, 379–388.
123 S. J. Sung, S. H. Min, K. Y. Cho, S. Lee, Y. J. Min, Y. I. Yeom and J. K. Park, *Biol. Pharm. Bull.*, 2003, **26**, 492–500.
124 A. Vonarbourg, C. Passirani, P. Saulnier and J. P. Benoit, *Biomaterials*, 2006, **27**, 4356–4373.
125 J. Y. Wong, T. L. Kuhl, J. N. Israelachvili, N. Mullah and S. Zalipsky, *Science*, 1997, **275**, 820–822.
126 R. S. Burke and S. H. Pun, *Bioconjugate Chem.*, 2008, **19**, 693–704.
127 S. Mishra, P. Webster and M. E. Davis, *Eur. J. Cell Biol.*, 2004, **83**, 97–111.
128 J. Shin, P. Shum and D. H. Thompson, *J. Controlled Release*, 2003, **91**, 187–200.
129 R. Tomlinson, J. Heller, S. Brocchini and R. Duncan, *Bioconjugate Chem.*, 2003, **14**, 1096–1106.
130 N. Murthy, J. Campbell, N. Fausto, A. S. Hoffman and P. S. Stayton, *J. Controlled Release*, 2003, **89**, 365–374.
131 R. S. Greenfield, T. Kaneko, A. Daues, M. A. Edson, K. A. Fitzgerald, L. J. Olech, J. A. Grattan, G. L. Spitalny and G. R. Braslawsky, *Cancer Res.*, 1990, **50**, 6600–6607.
132 M. Morille, C. Passirani, A. Vonarbourg, A. Clavreul and J. P. Benoit, *Biomaterials*, 2008, **29**, 3477–3496.
133 H. C. Guo, R. Z. Hao, H. S. Qian, S. Q. Sun, D. H. Sun, H. Yin, Z. X. Liu and X. T. Liu, *Appl. Microbiol. Biotechnol.*, 2012, **95**, 1253–1263.
134 P. Sharma, S. Brown, G. Walter, S. Santra and B. Moudgil, *Adv. Colloid Interface Sci.*, 2006, **123**, 471–485.
135 A. J. Mueller, D. U. Bartsch, U. Schaller, W. R. Freeman and A. Kampik, *Int. Ophthalmol.*, 2001, **23**, 385–393.
136 L. Wang, J. Liu, Y. Dai, Q. Yang, Y. Zhang, P. Yang, Z. Cheng, H. Lian, C. Li, Z. Hou, P. Ma and J. Lin, *Langmuir*, 2014, **30**, 13042–13051.
137 G. Chen, H. Agren, T. Y. Ohulchanskyy and P. N. Prasad, *Chem. Soc. Rev.*, 2015, **44**, 1680–1713.
138 F. Wang, R. Deng, J. Wang, Q. Wang, Y. Han, H. Zhu, X. Chen and X. Liu, *Nat. Mater.*, 2011, **10**, 968–973.
139 F. Zhang, R. Che, X. Li, C. Yao, J. Yang, D. Shen, P. Hu, W. Li and D. Zhao, *Nano Lett.*, 2012, **12**, 2852–2858.
140 F. Vetrone, R. Naccache, V. Mahalingam, C. G. Morgan and J. A. Capobianco, *Adv. Funct. Mater.*, 2009, **19**, 2924–2929.
141 G. Y. Chen, T. Y. Ohulchanskyy, S. Liu, W. C. Law, F. Wu, M. T. Swihart, H. Agren and P. N. Prasad, *ACS Nano*, 2012, **6**, 2969–2977.
142 P. Huang, W. Zheng, S. Y. Zhou, D. T. Tu, Z. Chen, H. M. Zhu, R. F. Li, E. Ma, M. D. Huang and X. Y. Chen, *Angew. Chem., Int. Ed.*, 2014, **53**, 1252–1257.
143 W. Zou, C. Visser, J. A. Maduro, M. S. Pshenichnikov and J. C. Hummelen, *Nat. Photonics*, 2012, **6**, 560–564.

144 Z. Q. Li, Y. Zhang and S. Jiang, *Adv. Mater.*, 2008, **20**, 4765–4769.
145 H. Zhang, Y. J. Li, I. A. Ivanov, Y. Q. Qu, Y. Huang and X. F. Duan, *Angew. Chem., Int. Ed.*, 2010, **49**, 2865–2868.
146 A. Barhoumi, Q. Liu and D. S. Kohane, *J. Controlled Release*, 2015, **219**, 31–42.
147 M. K. Jayakumar, A. Bansal, B. N. Li and Y. Zhang, *Nanomedicine*, 2015, **10**, 1051–1061.
148 H. C. Guo, D. Yan, Y. Q. Wei, S. C. Han, H. S. Qian, Y. S. Yang, Y. P. Zhang, X. T. Liu and S. Q. Sun, *PLoS One*, 2014, **9**, e112713.
149 O. O. Cirli and V. Hasirci, *J. Controlled Release*, 2004, **96**, 85–96.
150 L. J. Cai, J. B. Li, S. P. Wang, M. Z. Zhao, B. G. Zhao, C. L. Jiang and W. Kong, *Chem. Res. Chin. Univ.*, 2017, **33**, 294–297.
151 X. J. Zhang and R. X. Zhuo, *Macromol. Chem. Phys.*, 2016, **217**, 1934–1940.
152 W. Li, X. P. Zeng, H. Wang, Q. Wang and Y. J. Yang, *New J. Chem.*, 2016, **40**, 4528–4533.
153 G. Liu, W. Liu and C. M. Dong, *Polym. Chem.*, 2013, **4**, 3431–3443.
154 H. F. Li, K. Guo, C. Wu, L. Shu, S. W. Guo, J. Hou, N. P. Zhao, L. X. Wei, X. B. Man and L. Zhang, *Chem. Biol. Drug Des.*, 2015, **86**, 783–794.
155 H. I. Lee, W. Wu, J. K. Oh, L. Mueller, G. Sherwood, L. Peteanu, T. Kowalewski and K. Matyjaszewski, *Angew. Chem., Int. Ed.*, 2007, **46**, 2453–2457.
156 J. Q. Jiang, X. Tong, D. Morris and Y. Zhao, *Macromolecules*, 2006, **39**, 4633–4640.
157 E. Cabane, V. Malinova, S. Menon, C. G. Palivan and W. Meier, *Soft Matter*, 2011, **7**, 9167–9176.
158 R. Tong, H. D. Hemmati, R. Langer and D. S. Kohane, *J. Am. Chem. Soc.*, 2012, **134**, 8848–8855.
159 D. P. Ferris, Y. L. Zhao, N. M. Khashab, H. A. Khatib, J. F. Stoddart and J. I. Zink, *J. Am. Chem. Soc.*, 2009, **131**, 1686–1688.
160 J. Q. Jiang, B. Qi, M. Lepage and Y. Zhao, *Macromolecules*, 2007, **40**, 790–792.
161 N. K. Mal, M. Fujiwara, Y. Tanaka, T. Taguchi and M. Matsukata, *Chem. Mater.*, 2003, **15**, 3385–3394.
162 A. P. Goodwin, J. L. Mynar, Y. Ma, G. R. Fleming and J. M. Frechet, *J. Am. Chem. Soc.*, 2005, **127**, 9952–9953.
163 Y. Yang, F. Liu, X. Liu and B. Xing, *Nanoscale*, 2013, **5**, 231–238.
164 X. Wang, K. Liu, G. Yang, L. Cheng, L. He, Y. Liu, Y. Li, L. Guo and Z. Liu, *Nanoscale*, 2014, **6**, 9198–9205.
165 L. Wang, C. Gao, K. Liu, Y. Liu, L. Ma, L. Liu, X. Du and J. Zhou, *Adv. Funct. Mater.*, 2016, **26**, 3480–3489.
166 J. Shen, G. Chen, A. M. Vu, W. Fan, O. S. Bilsel, C. C. Chang and G. Han, *Adv. Opt. Mater.*, 2013, **1**, 644–650.
167 X. Xie, N. Gao, R. Deng, Q. Sun, Q. H. Xu and X. Liu, *J. Am. Chem. Soc.*, 2013, **135**, 12608–12611.
168 L. Liang, X. Xie, D. T. Loong, A. H. All, L. Huang and X. Liu, *Chem.–Eur. J.*, 2016, **22**, 10801–10807.
169 X. Li, Z. Guo, T. Zhao, Y. Lu, L. Zhou, D. Zhao and F. Zhang, *Angew. Chem., Int. Ed.*, 2016, **55**, 2464–2469.
170 Q. Chen, X. Xie, B. Huang, L. Liang, S. Han, Z. Yi, Y. Wang, Y. Li, D. Fan, L. Huang and X. Liu, *Angew. Chem., Int. Ed.*, 2017, **56**, 7605–7609.
171 H. S. Choi, W. Liu, P. Misra, E. Tanaka, J. P. Zimmer, B. Itty Ipe, M. G. Bawendi and J. V. Frangioni, *Nat. Biotechnol.*, 2007, **25**, 1165–1170.
172 L. Xiong, T. Yang, Y. Yang, C. Xu and F. Li, *Biomaterials*, 2010, **31**, 7078–7085.
173 L. Cheng, K. Yang, M. Shao, X. Lu and Z. Liu, *Nanomedicine*, 2011, **6**, 1327–1340.
174 D. M. Xu, S. D. Yao, Y. B. Liu, K. L. Sheng, J. Hong, P. J. Gong and L. Dong, *Int. J. Pharmacol.*, 2007, **338**, 291–296.
175 R. Nakaoka, Y. Tabata, T. Yamaoka and Y. Ikada, *J. Controlled Release*, 1997, **46**, 253–261.
176 S. M. Moghimi, A. C. Hunter and J. C. Murray, *Pharmacol. Rev.*, 2001, **53**, 283–318.
177 S. M. Moghimi, *Adv. Drug Delivery Rev.*, 1995, **17**, 61–73.
178 M. Gaumet, A. Vargas, R. Gurny and F. Delie, *Eur. J. Pharm. Biopharm.*, 2008, **69**, 1–9.
179 T. Banerjee, S. Mitra, A. Kumar Singh, R. Kumar Sharma and A. Maitra, *Int. J. Pharmacol.*, 2002, **243**, 93–105.
180 S. M. Moghimi, *Adv. Drug Delivery Rev.*, 1995, **17**, 103–115.
181 Y. Takakura, R. I. Mahato and M. Hashida, *Adv. Drug Delivery Rev.*, 1998, **34**, 93–108.
182 A. Bolbat and C. Schultz, *Biol. Cell.*, 2017, **109**, 1–23.
183 D. Hoglinger, A. Nadler, P. Haberkant, J. Kirkpatrick, M. Schifferer, F. Stein, S. Hauke, F. D. Porter and C. Schultz, *Proc. Natl. Acad. Sci. U. S. A.*, 2017, **114**, 1566–1571.
184 M. Schifferer, D. A. Yushchenko, F. Stein, A. Bolbat and C. Schultz, *Cell Chem. Biol.*, 2017, **24**, 525–531.
185 D. D. Li, Y. P. Zhang, Z. Y. Fan, J. Chen and J. H. Yu, *Chem. Sci.*, 2015, **6**, 6097–6101.
186 Y. Mu, N. Wang, Z. C. Sun, J. Wang, J. Y. Li and J. H. Yu, *Chem. Sci.*, 2016, **7**, 3564–3568.
187 G. Feng, P. Cheng, W. Yan, M. Boronat, X. Li, J. H. Su, J. Wang, Y. Li, A. Corma, R. Xu and J. Yu, *Science*, 2016, **351**, 1188–1191.

